Effect of Number of Digits on Human Precision Manipulation Workspaces

Thomas Feix, *Member, IEEE,* Ian M. Bullock, *Member, IEEE*, Yuri Gloumakov, *Student Member, IEEE,* and Aaron M. Dollar, *Senior Member, IEEE*

***Abstract*— Precision manipulation, or moving small objects held in the fingertips, is likely the most heavily utilized class of dexterous within-hand manipulation and adds greatly to the capabilities of the human hand. The present work focuses on studying the effects of varying the number of digits used on the resulting manipulation abilities, in terms of translational workspaces and rotational ranges, by manipulating two circular objects, 50 mm and 80 mm in diameter. In general, as the number of digits in contact with the object increases, the results show a significant reduction in precision manipulation workspace range for four of the six translation and rotation directions and no significant change in the other two, suggesting that for these particular metrics, more fingers result in a reduction in performance. Furthermore, while two digits results in the largest workspaces for five of the six translation and rotation axes, the lack of ability to control rotation in the distal-proximal direction suggests that three digits may be more desirable for overall precision manipulation dexterity.**

***Index Terms*— Dexterous Manipulation, Human Hands**

I. Introduction

The dexterity of the human hand is second to none, but the specific arrangement of a thumb and four fingers derives from constraints inherent within human evolutionary history and has not arrived at a globally optimal configuration. However, the development of artificial hands, such as within the robotics and prosthetics research communities, is not bound by the constraints of evolution or biology (although engineered systems have their own challenging limitations). And while an anthropomorphic configuration has certain benefits related to the "look" of an artificial hand, there are a number of reasons to consider alternative configurations, especially for options with much lower mechanical complexity – the human hand has at least 21 controllable degrees of freedom, at least 18 joints (almost all of which are multi-DOF, either active or passive), an incredibly complex tendon array to transmit actuation primarily from the forearm, and tens of thousands of sensors - all making it essentially impossible and certainly impractical to replicate in a robotic or prosthetic hand.

As an exercise to help lend insight into the tradeoffs of the anthropomorphic hand configuration, as well as an interesting line of investigation in its own right, we are undertaking a number of efforts to quantify human hand performance during functional tasks. In this paper, we seek to examine one key aspect of that question by investigating the role of number of digits on the ability of human subjects to translate and rotate objects held between the fingertips (Fig. 1 shows an example of this motion). This type of dexterous within-hand manipulation is often referred to as "precision manipulation", and is perhaps the most heavily utilized and important mode of within-hand manipulation [1]. These movements are utilized to accomplish daily tasks such as picking up small objects off of surfaces, fine motions for alignment and insertion (e.g. keys), tipping cups for drinking, using cutlery such as cutting with a knife, writing, and many others.

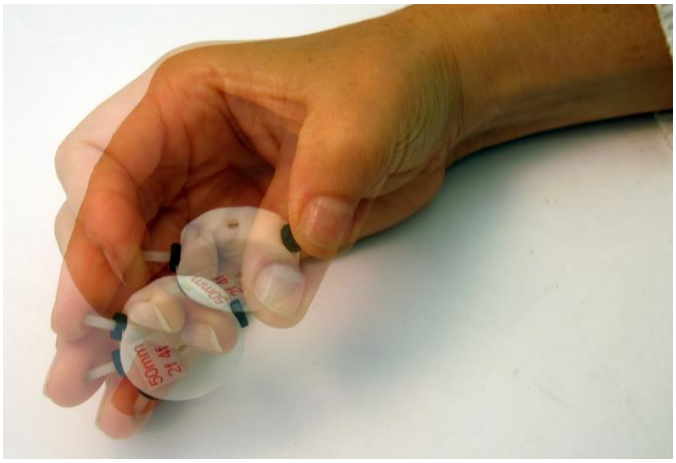

Figure 1. In this paper within-hand manipulation motions are considered, where an object is repositioned in the hand, without changing the contact location of the object. As indicated in the figure, the global position of the hand is not changed, all motion is evoked by finger movement.

In general, within-hand manipulation capabilities greatly add to the functionality of the human upper extremity, increasing precision and reducing the energy requirement compared to using the whole arm, allowing movements in constrained spaces, and adding to the total usable translational and rotational range of grasped objects. Aside from the previously mentioned applications inspiring robotic and prosthetic hand designs, we believe this work has applications in hand functional evaluation for rehabilitation (suggesting a potential methodology and presenting normative results), in providing a

Portions of this work were presented at the 2015 IEEE Engineering in Medicine and Biology Conference [19], [20]. This work was supported in part by the National Science Foundation grants IIS-1317976 and IIS-0953856.

Thomax Feix, Ian M. Bullock, Yuri Gloumakov, and Aaron M. Dollar are or were with Yale University ({thomas.feix, ian.bullock, yuri.gloumakov, aaron.dollar}@yale.edu), New Haven, CT, 06511.

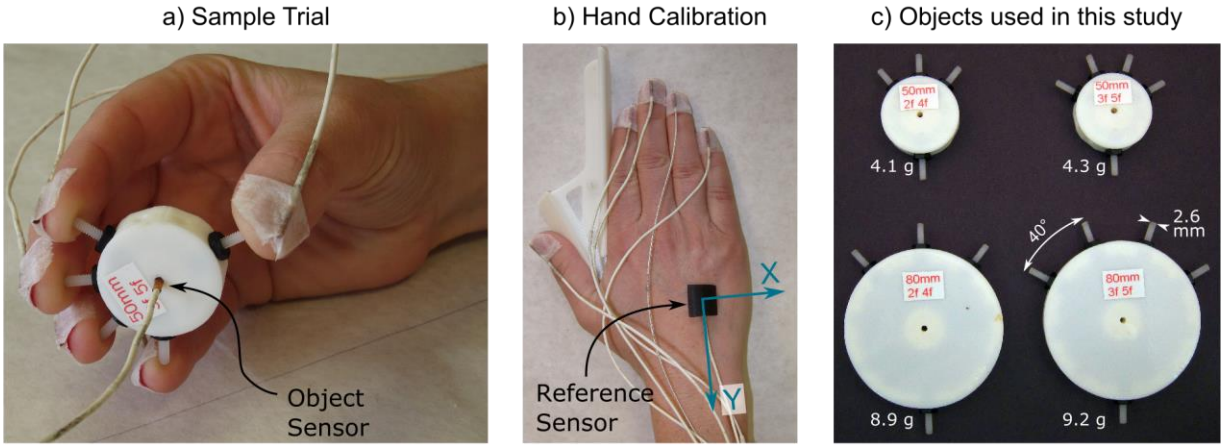

Figure 2. a) Sample trial of the 5 digit case with the 50 mm object. The object sensor is placed in the center of the object and the fingertips are used to grasp the five pointed contact locations of the object. b) The hand in the calibration setup, including the reference frames. This step is important as it defines the rotational axes. c) The four objects used in this study and their properties. The small objects have a diameter of 50mm (including the screw lengths), whereas the large object is 80 mm.

performance comparison to help benchmark the function of artificial hands against human capabilities insight for anthropology in terms of the evolution of human manual dexterity [2], and in primatology as a human baseline for comparison of primate manipulative capabilities [3], among others. Facilitating benchmarking for the robotics and prosthetics research communities, as the workspace sizes, shapes, and positions/orientations can serve as a comparison point for both anthropomorphic and non-anthropomorphic hand designs [4]–[10].

Analyzing human precision manipulation capabilities (i.e. grasped in the fingertips) can help provide benchmarks and inspiration for prosthetic and robotic hand design [11]–[15]. For hand rehabilitation it enables the pinpointing of critical movements that are important for normal hand function [16]. Haptic interfaces, such as those used in surgical robots [17], will also profit as human capabilities and behaviors are better understood. The work also will allow designers to align the workspace of their devices to the human dexterous workspace, improving overall performance [18]. This work can also provide insight into the number of digits that should be used for such a device.

We particularly focus this work on quantifying the range of motion and principle movement directions for rotation and translation of two sizes of disk objects grasped in the fingertips using two to five digits (Fig. 2). The presented work significantly extends the authors' preliminary work presented at the IEEE EMBC conference [19], [20], with a greatly expanded range of conditions and analysis for both the translational and rotational workspaces as well as a new look into the differences between them. We begin with a more thorough description of how this work fits within related work in the literature (section II), and then describe our experimental methodology (section III). We then present the experimental results (section IV) and a discussion of their interpretation (section V), ending with conclusions and future work (section VI).

II. Background

Few existing works have quantitatively examined human hand functional capabilities. Of these, the majority have examined *grasping* function, in which the hand is largely static after acquiring the object (e.g. [12], [13]). Even less attention has been given to hand function involving manipulation of grasped objects within the hand, generally referred to as in-hand manipulation or within-hand manipulation [1]. This functionality essentially differentiates human dexterous capabilities from that of other species, and is also more challenging to execute in robotic or prosthetic systems.

Prior research has focused on examining the positional workspace of human hands, in particular of the thumb and index finger. Approaches to determining the thumb-index workspaces included intersecting the free motion workspaces of thumb and index finger [21] and fit shapes into the workspace [22]. Previous work from the authors has analyzed overall workspace shape and size for two or three digits [11], with this study extending previous work by considering multiple object sizes and the effect of using four and five digits during manipulation. In particular it also analyzes the shape of those translational workspaces and provides insights for how the object is actually rotated. It should be noted that the existing literature studying fingertip forces, such as to better understand motor control or finger dynamics [23], is much more extensive than the kinematic approach taken in this work – for a review of the force-centric approach see [24], [25].

It has been shown that the number of digits used changes with the size and mass of the object [26], [27]. In that respect, adding more fingers increases the hands' ability to resist forces and grasp larger objects. Also, the individual contact forces are regulated with the goal to minimize the overall force, while maintaining stability [28]. In a five digit grasp, the forces of the individual digits are different, contributing to shear and normal forces in different amounts. Our research adds to this existing knowledge of how the number of digits affects capabilities of a hand.

III. Methods

Unimpaired human participants used their fingertips to manipulate objects of different sizes with a varying number of digits. If the standard numbering of the thumb, index, middle, ring, and pinky fingers as digits 1, 2, 3, 4, and 5 respectively is used, then the n-finger case involves using digits 1 through n. For example, the two-digit case involves using digits 1 to 2, or the thumb and the index finger. A magnetic tracker sensor in the object records workspace and angle points relative to a reference frame sensor on the back of the participant's hand (Fig. 2, with coordinate frame shown in 2b). Subjects were instructed to either move the object within their hand to explore the translation workspace or rotate the object back and forth while exploring their rotational range around a particular axis. The study was approved by the local IRB, and all participants were individually consented and financially compensated for participation.

A. Participants

16 participants (11 female, 5 male) completed the translational tasks and 17 participants (7 female, 10 male) completed the rotational tasks using circular objects of sizes 50 mm and 80 mm in diameter (Fig. 1). Participants had a median hand length, measured from wrist crease to middle fingertip, of 17.8 and 18.1 cm, respectively. The experimental setup required right-handed subjects, and any participants with significant prior hand or wrist injuries were excluded. Members of the authors' research group were also excluded from participation.

B. Equipment

A magnetic tracking system with 1.4 mm RMS positional accuracy and 0.5º RMS angular accuracy was used to measure object position and angle relative to a hand reference frame (trackSTAR system, Ascension Technologies, Burlington VT). A medium range transmitter (MRT) and ruggedized MODEL 180 2 mm diameter cylindrical sensors were used. Each sensor provides full 6 DOF data (*x*, *y*, and *z* position and rotation matrix) at 80 Hz. One sensor is fixed in the object using a nylon setscrew, and a reference frame sensor is placed in a small rubber sleeve and adhered to the back of the hand (along the 4th metacarpal) using Top Stick® Men's Grooming Tape.

Fig. 2 shows the object and the configuration of the digit contact pins. Two object sizes and four finger conditions were used for this experiment. The objects, including contact pin length, are either 50 mm or 80 mm in diameter. The contact points are at 40º spacing for the fingers, matching the natural finger spacing observed in [29]. For each object diameter, an "odd" (3 and 5 digit) and "even" (2 and 4 digit) object variant are used, to ensure that the fingers directly oppose the thumb regardless of the number of fingers used. The 50 mm object mass is 4.1 g for the 2 and 4 digit version and 4.3 g for the 3 and 5 digit version. The 80 mm object has a mass of 8.9 g for the 2 and 4 finger version and 9.2 g for the 3 and 5 digit version. All objects use 4-40 nylon screws for the digit contact points, with 2.6 mm outer diameter, to provide "pointed" contact locations. Using a small contact diameter, the finger-object contact is similar to a point contact, preventing rolling. Slippage, however, cannot be completely prevented and can still occur. Objects are entirely plastic to prevent any interference with the magnetic tracker measurements.

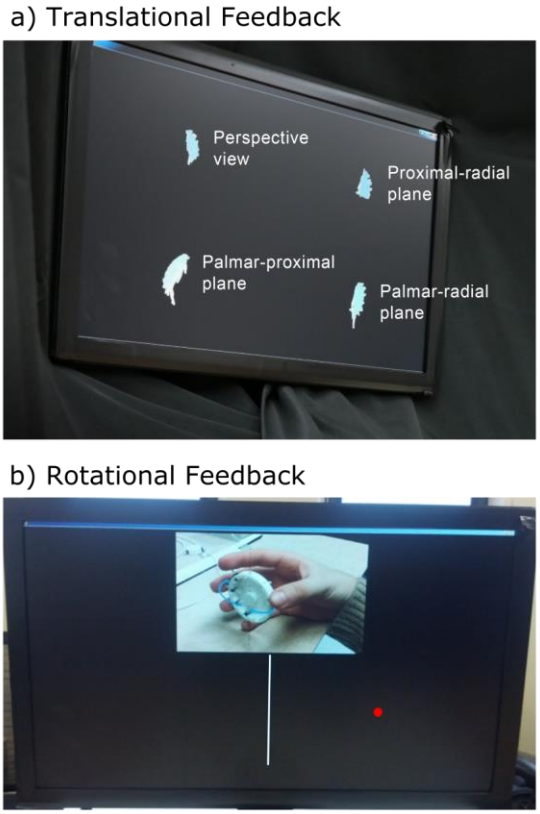

Figure 3. Visual feedback setup. A 27" monitor 1.5 m in front of the experimental table is used for feedback. a) For the translational study the workspace explored is shown to the participants in four different views – in three planes aligned with the hand axes, and one perspective view. (The text labels are shown here for explanatory purposes – no text was displayed during the study.) b) For the rotational study the top image on the feedback screen indicates the rotation the subject is supposed to perform during the experiment. The red dot indicates the current rotation around the given axis and the white line indicates zero. The subject is asked to move the point left and right by rotating the object.

A 27-inch (68.5 cm diagonal) LCD monitor 1.5 m in front of the experimental table provides visual feedback to participants. For the translational trials this screen displays the 3D object workspace in three orthogonal views aligned with the anatomical hand axes, as well as one perspective view (Fig. 3). The goal of the participant is to expand and fill the volume as much as possible, without breaking the contact on the fingertips. For the rotational trials the top part of the screen shows an image indicating the particular rotation axis for a particular trial. The bottom part shows a red dot representing the current rotation, while a white vertical line represents the zero angle position (Fig. 3, bottom). Depending on the trial, the subject had to rotate the object around one of the major axes (Fig. 4). It is important to note that the screen provides only feedback on the projected rotation around the goal axes, therefore rotating the object around axes other than the requested on will not provide significant rotations (see section III. F for details). We deliberately chose not to show information regarding previously explored rotational range (e.g. showing the highest achieved rotation so far in this trial), as this might have introduced a bias into our analysis. Not providing them any clues on their previous rotations allowed

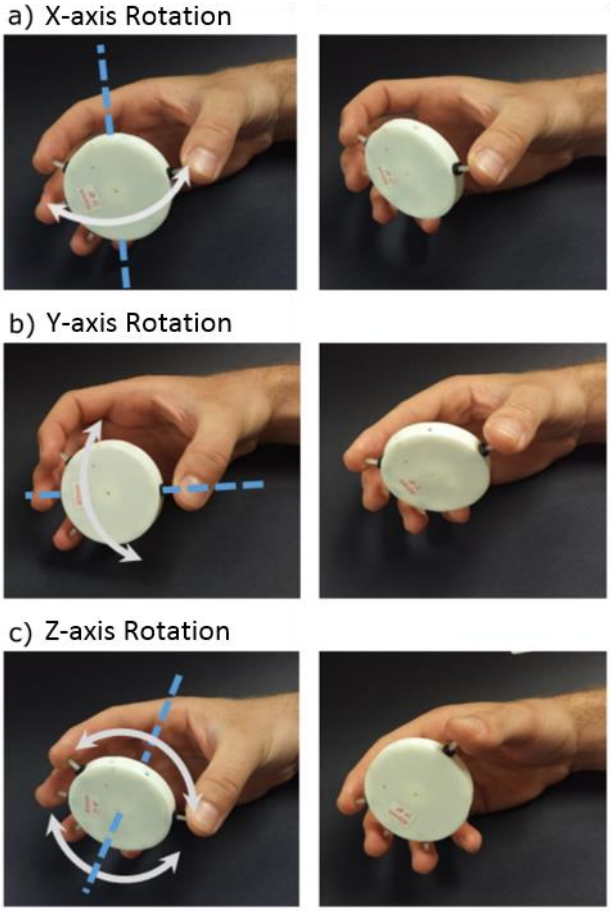

Figure 4. Images indicating the three rotation directions that were used in this study. For each rotation two images (left and right) are given, indicating roughly the two extreme conditions of the motion. Note that the exact axis of rotation is defined by the coordinate frame established by the reference sensor.

the participants to focus on exploring their actual kinematic limits.

The trakSTAR control and recordings were operated using Matlab R2014b on a Windows 7 operating system. Data management and statistical calculations were performed using Matlab R2019b.

C. Procedure

First, subjects were introduced to our experiment and the motions that we were interested in, translational or rotational. For those subjects undergoing the rotational trials, we showed sample videos of rotations around the three axes and explained the motions of the three different rotation conditions (see Fig. 4) for clarity. Then the hand proportions were measured while the hand laid flat on the table, including hand length (measured from the base of the hand near a wrist crease to the top of the middle finger) and hand width (measured between the two sides of the hand near the bases of the index finger and pinky). Afterwards the trakSTAR sensors were attached to the hand to track finger movements, as shown in Fig. 2. Double sided tape (Vapon Topstick® Men's Grooming Tape) was put onto the nail and the sensor was placed on it. Then 3M Transpore™ tape was placed on top of the sensor to further secure it. The reference sensor (Fig. 2), on the back of the hand was inserted into 1.5x1.5x0.3 cm rubber sleeve that was secured to the back of the hand with Vapon Topstick® Men's Grooming Tape. Additionally, 3M Transpore™ was put on top of the sleeve and about 1 cm of cable. The cables coming from the hand were fixated to the arm with loop straps and the cable was draped over the participant's shoulder, providing strain relief. The cable length was adjusted to prevent pulling on the sensors when closing the hand and to preclude the excess cable from interfering.

The object sensor was placed into a correctly spaced hole in the center of the object and was secured with a set screw. The object had to be changed depending on the trial, thus we ensured that the sensor was removable.

Two object sizes and (50 and 80 mm in diameter) and four digit conditions (2, 3, 4, and 5 digits) are used with two trials each. This totaled to 16 trials per person for the translation tasks. For the rotation tasks, subjects had to rotate the object about each of the orthogonal hand axes, leading to a total of 48 trials (3 rotation directions). During the trials, participants rest their hand on a flat surface with the back of their forearm and hand straightened against an alignment guide edge raised 6 mm above the table surface.

The translation task trials were organized in a randomized order, where each trial was repeated twice in succession. Participants are instructed to move the object in the fingertips and trace out as much area as possible on the monitor, thus exploring their manipulation workspace. They are instructed to minimize wrist movement, but small wrist movements are permissible since all object motions are referenced relative to a base sensor on the back of the hand. Before the actual trial, there was a training period where subjects could familiarize themselves with the particular trial condition and practice moving the object. Trials in which the object is dropped (6% of trials) are removed from the data for final analysis. These occasional drops show that maintaining stable object contact for a full two minute trial without external adjustments can be difficult.

The rotation task trials on the other hand were only 30 seconds in length with 10 seconds of rest in between and trials where drops or repositions occurred were not removed from the final analysis. This portion of the experiment was structured in two parts, where each part contains all 24 conditions in random order. To simplify the experiment, the three rotation conditions for a particular digit count and object size combination were done in one block, reducing the number of object changes. Prior to each block of 3 rotation trials there was a training period where subjects could familiarize themselves with the particular condition and practice rotating the object. On screen feedback was provided for all three rotations simultaneously during training. The subjects indicated when they were ready to start the experiment. Then the hand and object were calibrated for the three subsequent trials. The subjects were instructed to maintain contact between the ulnar side of the hand and the table to reduce skin motion under the reference sensor.

D. Object size normalization

We anticipate that most effects of interest will scale with the size of the hand, as it is has been shown to highly correlate with other physical features [30]. In our case, we expect that the size of the object relative to the size of the hand will better define how it is manipulated than the absolute size of the object. It is also important to include relative object size as a covariate in

the analysis since we could not control for hand size during the experiment. Obtaining the relative object size can be done by dividing the object length (or diameter) by either the hand length or width, which results in a variable representing the size of the object as a percent of the hand dimension. Thus, prior to calculating the relative object size, we first identified which hand dimension had a significant effect on the translation and rotation workspaces. By using relative object size as a variable, we are able to observe its effect on the volume without having to scale the volume for a cross subject analysis. Same is true for rotation amplitudes, where the hand size provides no direct scaling factor.

E. Volume Calculation

Workspace volumes are calculated using a voxel binning method, as in [11]. Specifically, the object workspace points are binned into a three dimensional grid of voxels with 2.15 mm length for each edge of the voxel cube, the edge length used in [11] is maintained. The overall volume is calculated as the sum of the voxel volumes that contain at least one data point.

F. Rotation Angle Calculation

The output from the trakSTAR is a 3x3 rotation matrix r that encodes the orientation of the object with respect to the hand coordinate frame. Based on this information, the orientation of the object with the three global coordinate axes is sought. We use an X-Y-Z fixed angle representation, a particular three-angle representation [31] of X(ψ), Y(θ), Z(ϕ):

$$\theta = atan2\left(-r_{31}, \sqrt{r_{11}^2 + r_{21}^2}\right)$$

$$\psi = atan2\left(\frac{r_{21}}{\cos\theta}, \frac{r_{11}}{\cos\theta}\right)$$

$$\phi = atan2\left(\frac{r_{32}}{\cos\theta}, \frac{r_{33}}{\cos\theta}\right)$$

For the X and Z rotation, the rotation angle can be between ±180 degrees and for Y the rotation ± 90 degrees to give the correct rotation. Angles beyond that either jump by 360 degrees (X, Z) or jump to a different solution (Y). Tests with simulated data confirmed that this representation allows the extraction of the three global rotation angles (see verification in Fig. A1 in Appendix). A rotation matrix is created by multiplying together individual rotation matrices along X, Y, and Z axes. To test for robustness of the angle calculation, the direction along which the rotation is measured (primary rotation) is kept the same while the two other rotations (secondary rotations) are given random noise. The extracted X, Y, and Z axis rotations from each rotation trial can be seen in Fig. A1. For each angle (from -180 to 180 degrees in 6 degrees steps) this is repeated 1000 times and the 90th percentile is used as error representation. Even when there is a noise of up to ±40 degrees, the estimation still works reliably, however the ranges that return meaningful data are reduced. The error magnitude in the primary rotation is always smaller than the amount of noise in the secondary rotations.

In the two digit trials, the object is only held at two points, therefore it is not fully constrained in space. The rotation around the axis connecting the two contact locations cannot be fully controlled; the object could potentially spin around this axis. During the experiments, we paid special attention to the cable of the object sensor, making sure it always pointed in the same direction. This way the cable from the object sensor was used to prevent excessive rotations. However, this only prevented the object from rotating by more than about 90 degrees.

G. Rotational Workspace Calculation

For each 30 s rotation trial the rotational workspace needs to be computed (for illustration, see Fig. A2 in Appendix). Therefore, the following steps are performed:

1) Detect the minima and maxima in the trial. We use the Matlab function "findpeaks" with the prominence parameter set to 1/8th of the total observed angular range. Using this function the extremes in the dataset are detected very reliably. The number of peaks (both maxima and minima) ranged from 6 peaks up to 99 peaks for the 30 s trial.

2) Check that the minima and maxima are alternating in the dataset. If not remove the second peak. Only 5 peaks had to be removed for the whole experiment.

3) Calculate the difference between min and max values of adjacent peaks. The vertical red lines in the left plot in Fig. A2 (in Appendix) indicate those differences. Using the peak differences avoids problems with drift, which occured in some trials.

4) Remove outliers and calculate the rotational amplitude by identifying the maximum difference between a pair of min and max rotational values. Outliers are detected beyond three standard deviations from the mean. We feel that looking at only the mean of the peak to peak differences could underestimate the maximal rotational range.

H. Calculation of Actual Rotation Axis

For the rotational trials we also calculated the axis around which the actual rotation occurred, which could potentially be different from the requested rotation axis. Based on the rotational workspace calculation, the indices i of the maxima and minima are extracted. Using those indices the rotational components S_i of the object center are extracted for those instances. In order to calculate the axis of rotation that rotates S_i to S_{i+1}, the body rotation matrices m_i are first extracted [32]

$$m_i = S_{i+1} S_i^T.$$

The rotation axis is extracted by calculating the eigenvectors of m_i, where the real eigenvector is the rotation axis that is sought. The average axis directions for each trial are computed by taking a simple average of the vectors in Euclidean space [31], after projecting the vectors into a single hemisphere to avoid any issues with averaging equivalent "negative" and "positive" versions of the same vector. The hemispheres are defined such that all X coordinates are positive for the rotation around X, all Y coordinates positive for rotations around Y and all Z coordinates positive for rotations around Z. As we can assume that the actual rotation axes will be close to the goal axis, this procedure guarantees that all rotation axes will point generally the same direction. The cone angle is then calculated as the half angle between the mean axis and the side of the cone, such that 68% of the axes lie within the cone. This provides an estimate about the spread of the data around the mean axis. This method is also discussed in [14].

I. Significance Testing

Factors for each experiment were tested for significance using an analysis of covariance (ANCOVA). This method, similar analysis of variance (ANOVA), looks to identify whether the independent categorical variables significantly affect the continuous response variable (workspace), while able to account simultaneously for covariates; covariate variables are continuous variables that may confound the statistical power of the categorical variables. No interaction effects were assumed between variables; a conservative assumption. Sex and diameter are considered as categorical variables, number of digits is ordinal, and hand length and width are the covariates. Relative object size, included in the follow up analyses, is also a covariate. Repeated measures were averaged to obtain a single performance value per subject, and the trial number in the analysis would refer to the order position of the second repetition. Each variable's p-value is then adjusted using a Holm-Bonferroni correction [33], to evaluate in more detail how individual factors affect the workspace while accounting for repeated testing. P-values accompanying the bottom of each table indicate whether the factors simultaneously (the model) affect the response variable. Two-tailed t-tests are used to further compare pairs of distributions within a single factor, such as number of digit conditions, while paired two-tailed t-tests are used to compare distributions that have paired observations, such as comparing the effect of different sized objects. A two-tailed t-test evaluates whether there exists a significant difference between the means of two distributions.

IV. Results

A. Translation Experiment

The translational experiment was completed by 16 subjects. Trials where the object was dropped were ignored, thus out of the maximum 256 trials only 240 were considered, and after averaging pairs of repeated trials, 125 trials remained; after dropped object trial omission, not all trials had a pair to average with. The average translational workspace over all conditions is 5.1 cm^3.

An ANCOVA was used to assess whether subject attributes and task conditions had an effect on the volume workspace (Table 1). An initial assessment of the adjusted p-values suggests that only the number of digits and hand width have a significant effect on the translation workspace. Due to the large range and significance of hand width, we omit hand length from the rest of the analysis and combine the hand width and diameter variables into a single variable representing the ratio of the two; object diameter divided by hand width, namely relative object size (Table 2). This new variable aggregates results from both object size trials while offering the readers results that generalize to any sized object. In the updated table, only the number of digits has a significant effect on volume.

Translation workspace is also analyzed by looking at the range of object translation along each the three major hand axes. Range is calculated as the difference between the maximum and minimum data along each direction. Similar to the rotational range analysis, we used a common outlier detection approach that identifies points beyond three standard deviations from the mean. Tables 3-5 analyze the effect of different trial conditions and relative object size (object diameter divided by hand width) on each translational direction using ANCOVA.

TABLE 1
ANALYSIS OF COVARIANCE: TRANSLATION VOLUME

volume ~ 1 + sex + hand len. + hand wid. + trial # + diameter + # of dig.

	SumSq	df	MeanSq	F	p-value	partial η^2	adjusted p-value
sex	34.0	1	34.0	3.72	0.056	0.031	0.168
hand length	9.87	1	9.87	1.08	0.301	0.009	0.601
hand width	99.5	1	99.5	10.9	0.001	0.086	0.006
trial number	42.6	1	42.6	4.67	0.033	0.039	0.131
diameter	4.1e-4	1	4.1e-4	4.5e-5	0.995	3.9e-7	0.995
# of digits	301.4	3	100.5	11.0	2.0e-6	0.222	1.2e-5
Error	1158.5	116	9.13				

Number of observations: 125, Root Mean Squared Error: 3.02
R-squared: 0.311, adjusted R-Squared: 0.263
F-statistic vs. constant model: 6.54, p-value = 5.07e-07

TABLE 2
ANALYSIS OF COVARIANCE: TRANSLATION VOLUME

volume ~ 1 + sex + relative object size + trial # + # of dig.

	SumSq	df	MeanSq	F	p-value	partial η^2	adjusted p-value
sex	10.7	1	10.7	1.09	0.298	0.009	0.596
relative size	3.56	1	3.56	0.363	0.548	0.003	0.596
trial number	42.8	1	42.8	4.38	0.039	0.036	0.116
# of digits	304.6	3	101.5	10.4	4.1e-7	0.20	1.7e-5
Error	1154.8	118	9.79				

Number of observations: 125, Root Mean Squared Error: 3.13
R-squared: 0.248, Adjusted R-Squared: 0.21
F-statistic vs. constant model: 6.49, p-value = 6.1e-06

TABLE 3
ANALYSIS OF COVARIANCE: X-DIRECTION TRANSLATION RANGE

range X ~ 1 + sex + relative object size + trial # + # of dig.

	SumSq	df	MeanSq	F	p-value	partial η^2	adjusted p-value
sex	10.5	1	10.5	5.40	0.022	0.004	0.065
relative size	0.032	1	0.032	0.017	0.897	1.4e-4	0.897
trial number	9.36	1	9.36	4.81	0.030	0.039	0.065
# of digits	57.2	3	19.1	9.80	8.0e-6	0.199	3.2e-5
Error	229.7	118	1.95				

Number of observations: 125, Root Mean Squared Error: 1.4
R-squared: 0.27, Adjusted R-Squared: 0.233
F-statistic vs. constant model: 7.28, p-value = 1.23e-06

TABLE 4
ANALYSIS OF COVARIANCE: Y-DIRECTION TRANSLATION RANGE

range Y ~ 1 + sex + relative object size + trial # + # of dig.

	SumSq	df	MeanSq	F	p-value	partial η^2	adjusted p-value
sex	0.515	1	0.515	0.383	0.537	0.003	1
relative size	0.227	1	0.227	0.169	0.682	0.001	1
trial number	7.14	1	7.14	5.31	0.023	0.043	0.092
# of digits	12.3	3	4.11	3.06	0.031	0.072	0.093
Error	158.4	118	1.34				

Number of observations: 125, Root Mean Squared Error: 1.16
R-squared: 0.122, Adjusted R-Squared: 0.0772
F-statistic vs. constant model: 2.73, p-value = 0.0162

TABLE 5
ANALYSIS OF COVARIANCE: Z-DIRECTION TRANSLATION RANGE

range Z ~ 1 + sex + relative object size + trial # + # of dig.

	SumSq	df	MeanSq	F	p-value	partial η^2	adjusted p-value
sex	0.051	1	0.051	0.077	0.782	6.5e-4	0.782
relative size	10.2	1	10.2	15.2	1.6e-4	0.114	4.8e-4
trial number	0.536	1	0.536	0.800	0.373	0.007	0.746
# of digits	16.6	3	5.52	8.25	5.0e-5	0.173	1.9e-4
Error	79.0	118	0.670				

Number of observations: 125, Root Mean Squared Error: 0.818
R-squared: 0.264, Adjusted R-Squared: 0.227
F-statistic vs. constant model: 7.05, p-value = 1.97e-06

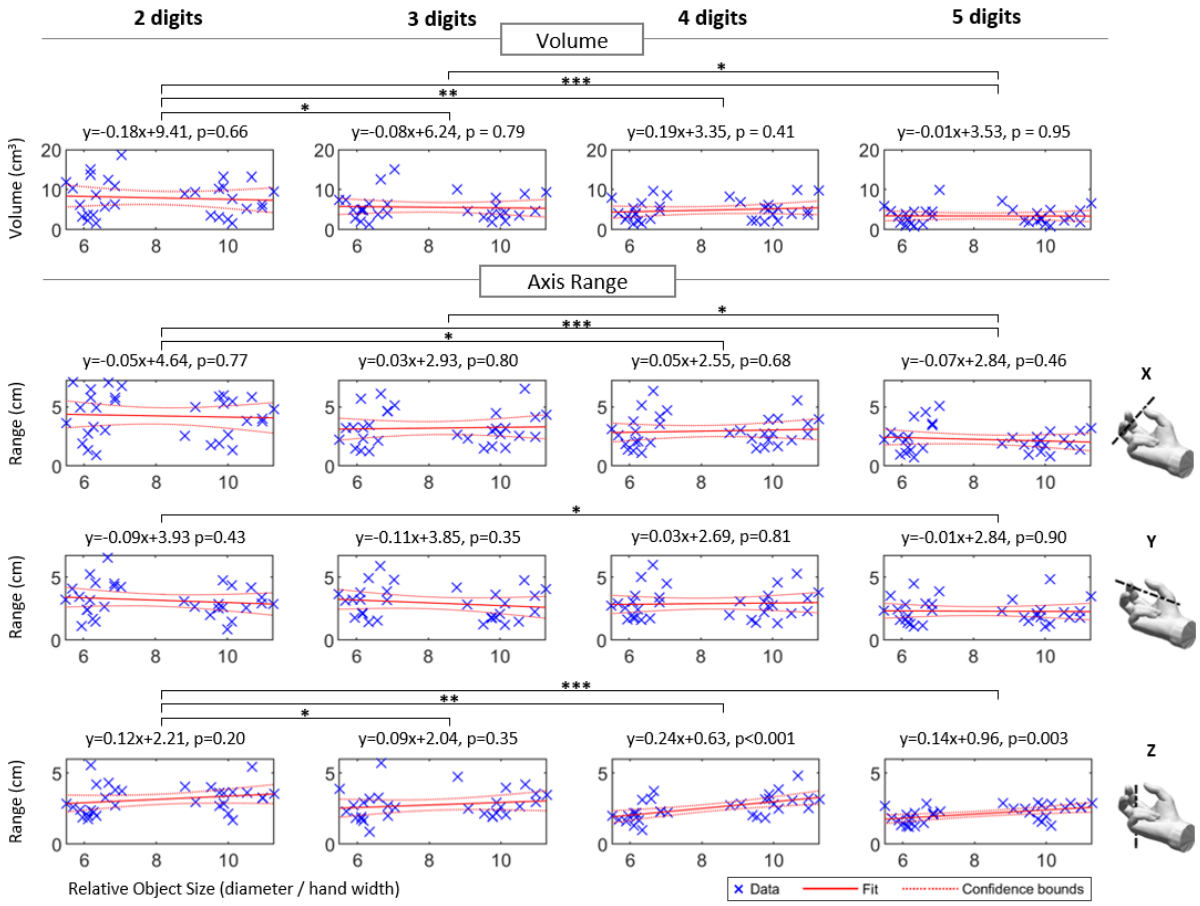

Figure 5. Overview of the translational workspace analyzed using both volume and range vs. relative object size (using hand width). The top row corresponds to the volume, whereas the bottom three rows correspond to range along each of the major axes (accompanied by a respective image). For each 3D translation exploration trial, the ranges along the three major hand axes are calculated. The three hand images on the right indicate the coordinate axes. The significance levels for the differences between pairs of distributions of trial conditions is given in the image: * denotes $p<0.05$, ** denotes $p<0.01$, and *** denotes $p<0.001$. For each trial condition, a regression is additionally calculated to identify whether a trend exists between the volume or range and the relative object size; results of which are displayed above each distribution.

The effect of the number of digits used on volume and range is evident, and we further investigate the effect of relative object size using a series of linear regressions for each digit condition (Fig. 5). The results indicate that the relative object size is not a significant variable for any of the digit cases for the overall volume. Of all conditions, relative object size was only a significant predictor of translation range along the Z direction for 4 and 5 digits. For these trial conditions, a larger object to hand width ratio was more likely to have a larger translational range. Finally, confirming the trends seen with volume, ranges generally decrease with added digits. The effect of the number of digits on volume and range for each of the diameter conditions separately is included in the Appendix for reference (Fig. A3 and Fig. A4).

An analogous analysis using hand length in lieu of hand width is included in the Appendix for reference for both workspace quantities; volume and range (Fig. A5 and Tables A1-A4). The analyses, using object diameter to hand length ratio as a variable, exhibited very similar results with similar takeaways.

Without accounting for other factors, although the male workspaces are 9% larger, the workspace distribution is not significantly different from female workspace distribution (p = 0.5, two-tailed t-test). Scaling the workspace for hand length, a sex effect is present, with female workspaces being 38% larger than male workspaces (p=0.026, two-tailed t-test). There is also a positive relationship between trial order and workspace (p = 0.014, 0.16 cm^3 increase per trial, linear fit of workspace vs. trial number), when not accounting for the other factors. The mean coefficient of variation (standard deviation/mean) for each object size and number of digits condition is 62% (49-74%).

To further analyze the shape of the translational workspaces, a Principal Component Analysis (PCA) of the workspace point cloud was performed. Results are shown in Fig. 6, which shows both the individual trials in the background and the overall mean direction for each trial condition. The mean direction was calculated as the Euclidean average over all individual PCs, similar to [11]. Additionally, Table A5 (in Appendix) presents summary statistics of the point cloud position and PC directions. For both object sizes the first PC (PC1) is the most stable, therefore For the 50 mm object there is a dominant direction that is mainly visible in the palmar/proximal plane, where most axes are aligned. With added number of fingers, the dominant direction of the PC1 shifts toward the little finger, both in the radial/proximal and palmar/ulnar plane. The 80 mm object shows a different trend; there is a larger variability between trials, the cone angle of PC1 is always larger than the

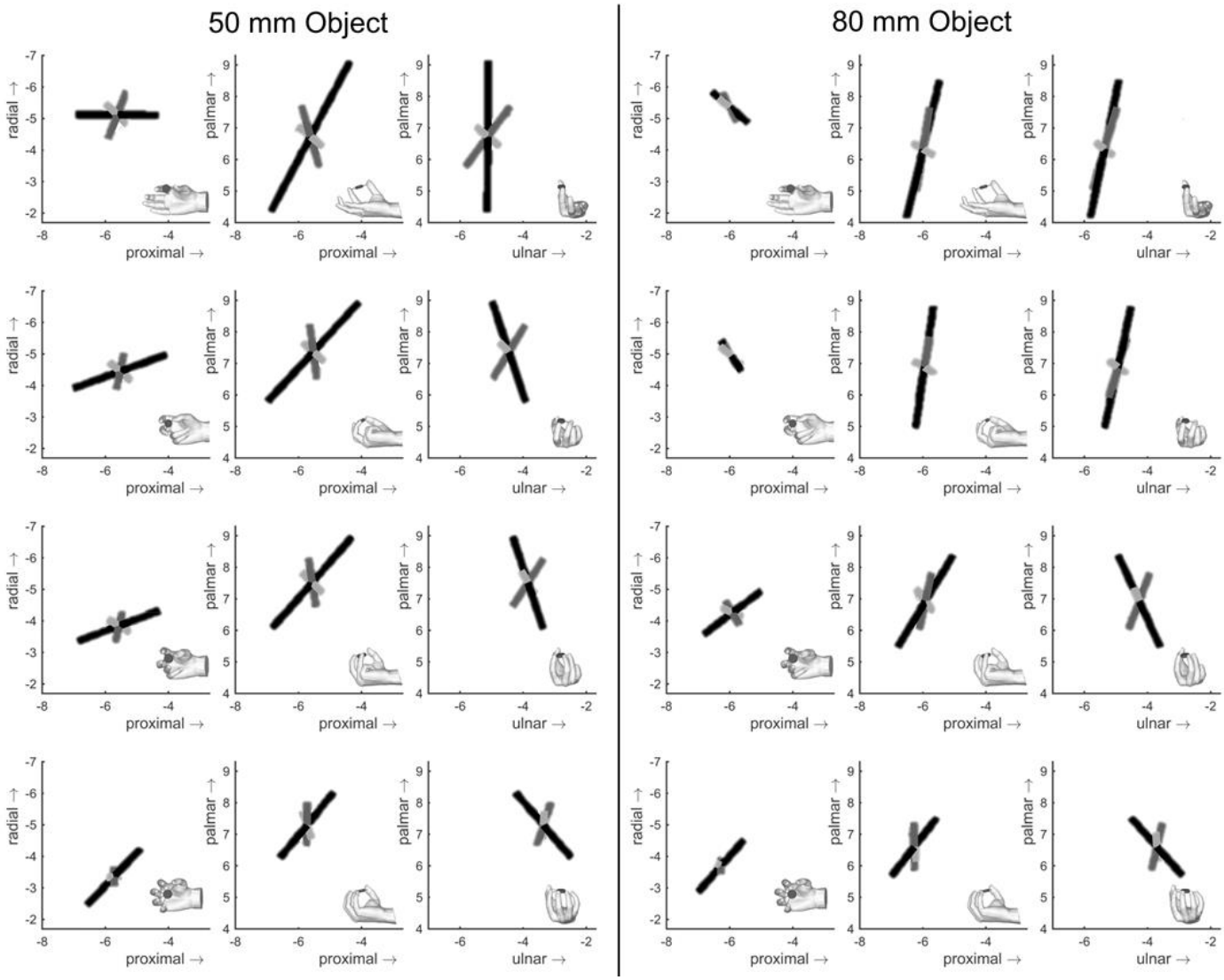

Figure 6. Principal components for all experiment conditions. Principal components analysis is used to find an orientation for three principal vectors for each participant's workspace. The average of all participants' PCA vectors is plotted as the thick set of lines, whereas the individual subjects' PC1 lines are plotted in the background. The length of these vectors is set by extending the axes 1.96σ in either direction. Each row corresponds to a digit condition, starting with the 2 digit condition on top, ending with the 5 digit condition at the bottom. Each set of three horizontal panels correspond to orthogonal views of the same task condition.

50 mm counterpart (Table A5). There is the tendency that the direction of the PC gradually shifts towards the pinky as fingers are added. Even though the orientations of the PCs' are less stable for the 80 mm object, the workspace does not become more uniform in shape. The relative lengths of PC1 to PC2 and PC1 to PC3 is generally constant at around 2.2 (1.7 – 2.4) and 4.9, respectively (3.9 – 5.9).

B. Rotation Experiment

The rotation experiment was completed by 17 subjects with 792 trials overall. The first two subjects did not perform the 2 digit trials, and since the rest of the experiment protocol was the same they were not excluded. The average rotational range over all conditions is 55 degrees with a standard deviation of 26 degrees. The largest rotational range is achieved in the 3 digit Y rotation with a mean rotation amplitude of 88 degrees and standard deviation of 28 degrees.

An ANCOVA was calculated to predict each of the rotational ranges based on subject attributes and task conditions (Tables 6-8). Although all measured a rotation workspace, each rotation task was analyzed independently due to different task goals. By controlling for the inter-subject variabilities, using Holm-Bonferroni p-value correction, we are able to observe whether specific task conditions (i.e. sex, number of digits, relative object size, and trial number) had an effect on each rotational range. Relative object size variable represents the ratio of object diameter to hand length. When evaluating ANCOVA using diameter, hand length, and width as separate variables, unlike for the translation trials, hand length had a significant effect on the rotational ranges while hand width did not (see Tables A6-A8 in Appendix). ANCOVA analyses suggest that the relative size of the object has a significant effect on the rotational range for all conditions, particularly around the X and the Z axes. The number of digits used was only significant when rotating the object around the Y-axis.

As a follow up to the ANCOVA analysis, we further explored the effect of the number of digits and relative object size on each rotational range using a series of single factor ANOVA and a series of linear regressions, respectively (Fig. 7); significant

TABLE 6
ANALYSIS OF COVARIANCE: X-AXIS ROTATION RANGE

range X ~ 1 + sex + relative object size + trial # + # of dig.

	SumSq	df	MeanSq	F	p-value	partial η^2	adjusted p-value
sex	423	1	423	1.74	0.190	0.014	0.569
relative size	3960	1	3960	16.3	9.5e-5	0.115	3.8e-4
trial number	11.3	1	11.3	0.046	0.830	3.7e-4	0.830
# of digits	956	3	319	1.31	0.274	0.030	0.569
Error	30436	125	244				

Number of observations: 132, Root Mean Squared Error: 15.6
R-squared: 0.159, Adjusted R-Squared: 0.119
F-statistic vs. constant model: 3.94, p-value = 0.0012

TABLE 7
ANALYSIS OF COVARIANCE: Y-AXIS ROTATION RANGE

range Y ~ 1 + sex + relative object size + trial # + # of dig.

	SumSq	df	MeanSq	F	p-value	partial η^2	adjusted p-value
sex	1038	1	1038	2.47	0.119	0.019	0.237
relative size	4186	1	4186	9.96	0.002	0.074	0.006
trial number	21.3	1	21.3	0.051	0.822	4.1e-4	0.822
# of digits	58944	3	19648	46.8	2.5e-20	0.529	9.9e-20
Error	52528	125	420				

Number of observations: 132, Root Mean Squared Error: 20.5
R-squared: 0.559, Adjusted R-Squared: 0.537
F-statistic vs. constant model: 26.4, p-value = 4.19e-20

TABLE 8
ANALYSIS OF COVARIANCE: Z-AXIS ROTATION RANGE

range Z ~ 1 + sex + relative object size + trial # + # of dig.

	SumSq	df	MeanSq	F	p-value	partial η^2	adjusted p-value
sex	1164	1	1164	4.65	0.033	0.036	0.099
relative size	6273	1	6273	25.1	1.83e-6	0.167	7.3e-6
trial number	47.3	1	47.3	0.189	0.664	0.002	0.664
# of digits	1916	3	639	2.55	0.059	0.058	0.117
Error	31275	125	250				

Number of observations: 132, Root Mean Squared Error: 15.8
R-squared: 0.248, Adjusted R-Squared: 0.212
F-statistic vs. constant model: 6.87, p-value = 2.55e-06

differences between digit condition distributions are depicted above pairs of scatterplots. Object size evidently has a significant effect on the range of rotation, barring rotations made with 2 digits, with larger relative object size reducing the rotational range. The difference in the range of rotation distribution between digit conditions was only apparent in rotations around the Y-axis. When comparing trials by object size (without accounting for hand size), the median rotational range of the small object is 1.3, 1.2, and 1.2 times larger than the large object for X, Y, and Z, rotations, respectively ($p < 0.001$, $p = 0.009$, and $p < 0.001$, respectively (paired two-tailed t-test); consistent with the trends seen in Fig. 7. We further investigate the variables through a series of additional statistical tests.

Sex has an effect on the rotation ranges, with male workspaces being 12% larger, when considering all rotation conditions (reaffirmed with a two-tailed t-test, $p = 0.0006$). Even when dividing the rotational ranges by the individual hand lengths, male workspaces are still 7% larger ($p = 0.041$, two-tailed t-test). A similar hand width effect exists as in the translational analysis, with wider hands lowering the rotational range. Although insignificant when accounting for all variables, there is a positive relationship between trial order and workspace when considering the effect alone ($p = 0.022$, increase per trial 0.15 degrees, linear fit of range vs. trial number). The mean coefficient of variation (standard deviation/mean) for each object size/number of digit condition is 37% (18% - 66%). The three largest coefficients (66%, 49%, and 47%) are from two digit trials, the next largest is 44%.

To analyze the amount of translation motion when performing the rotations, PCA was performed on the positional coordinates of the object center. Since the experiment was a one dimensional exploration it is expected that the object center will

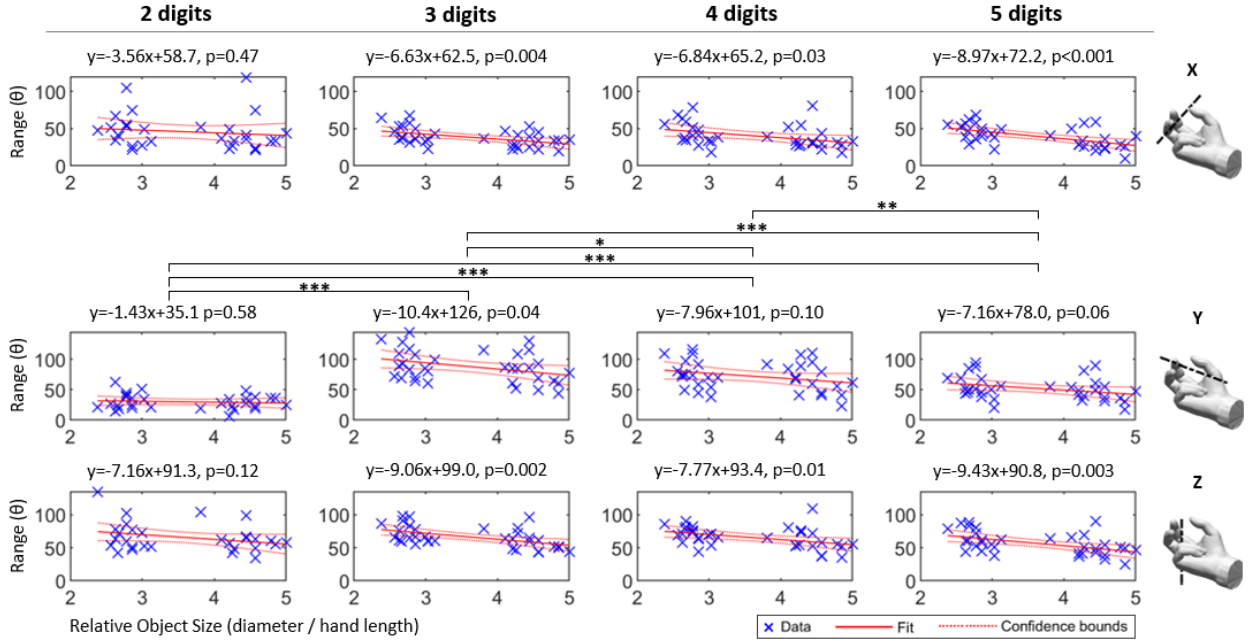

Figure 7. Overview of the rotational ranges for all 24 conditions. Each row, accompanied by an image, corresponds to a different rotation trial. The significance levels for the differences between number of digits is given in the image; * denotes $p<0.05$, ** denotes $p<0.01$, and *** denotes $p<0.001$. The three hand images on the right indicate the directions of the three rotations in the experiment. Each regression is accompanied with p-values describing the likelihood of the trend.

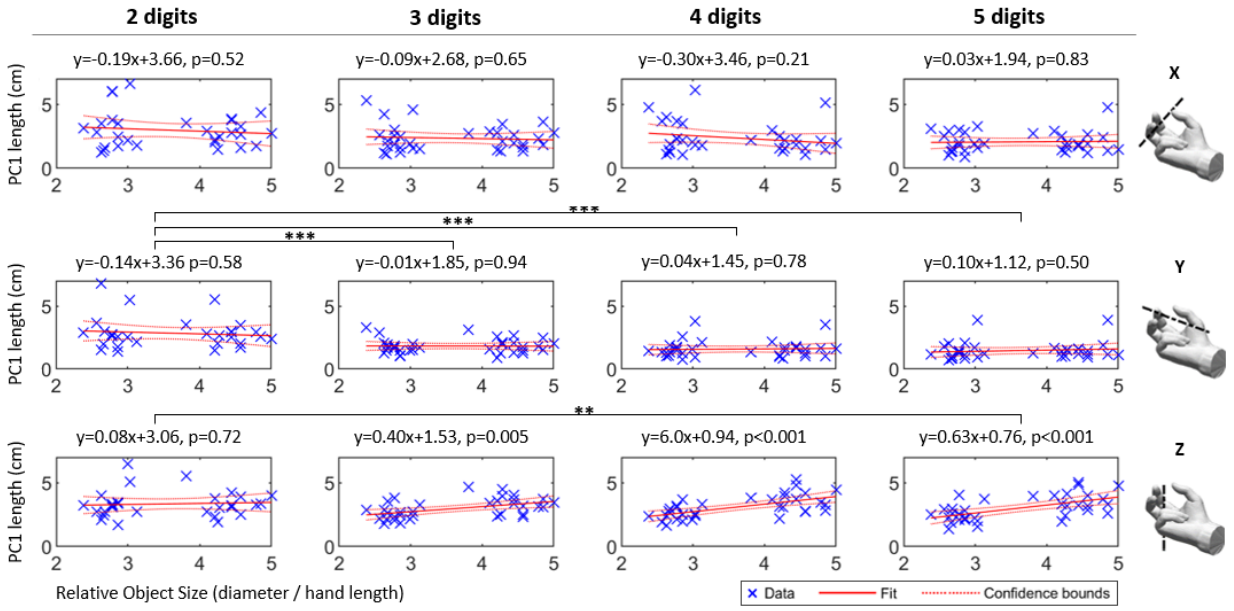

Figure 8. The figure shows the amount of translational travel of the object during the rotational trials. The length of these vectors is set by extending the axes 1.96σ in either direction. The three hand images on the right, corresponding to the row, indicate the directions of the three rotations in the experiment. * denotes $p<0.05$, ** denotes $p<0.01$, and *** denotes $p<0.001$, as to whether the means of the distributions are significantly different. Each regression is accompanied with p-values describing the likelihood of the trend.

lie on a narrow point cloud. Therefore, PC1 will capture the amplitude of the motion. Fig. 8 presents the length of PC1. The length of the axes is defined by a $\pm 1.96\sigma$ range for the data, the interval that statistically incorporates 95% of the data. Overall, the object moves around 2-3 cm in the rotation trials. The only noteworthy significant differences are 2 digit conditions that are larger compared to higher digit conditions, unsurprising given the challenge of rotating around the Y-axis using only 2 digits. Relative object size had a significant effect on the length of PC1 for only the Z-axis rotation trials for 3-5 digit cases.

TABLE 9
ACTUAL AXIS OF ROTATION STATISTICS

Digits		X	Y	Z
50 mm Object				
2	Mean Axis	(0.86, 0.44, 0.25)	(0.069, 1, 0.018)	(-0.27, -0.34, 0.9)
2	Cone Angle	31	29	13
2	Goal Angle	30	4.1	26
3	Mean Axis	(0.88, 0.21, 0.43)	(-0.25, 0.94, 0.21)	(-0.32, -0.14, 0.94)
3	Cone Angle	27	15	17
3	Goal Angle	28	19	21
4	Mean Axis	(0.93, 0.15, 0.33)	(-0.28, 0.92, 0.27)	(-0.15, -0.16, 0.97)
4	Cone Angle	21	17	12
4	Goal Angle	21	23	13
5	Mean Axis	(0.97, 0.16, 0.17)	(-0.35, 0.91, 0.22)	(-0.019, -0.23, 0.97)
5	Cone Angle	23	24	11
5	Goal Angle	13	25	14
80 mm Object				
2	Mean Axis	(0.92, 0.31, 0.24)	(0.044, 0.99, 0.091)	(-0.39, -0.52, 0.76)
2	Cone Angle	25	29	12
2	Goal Angle	23	5.8	40
3	Mean Axis	(0.94, -0.02, 0.35)	(-0.31, 0.91, 0.25)	(-0.46, -0.31, 0.83)
3	Cone Angle	32	15	12
3	Goal Angle	21	24	34
4	Mean Axis	(0.95, -0.06, 0.3)	(-0.31, 0.89, 0.32)	(-0.32, -0.36, 0.88)
4	Cone Angle	25	16	14
4	Goal Angle	18	27	29
5	Mean Axis	(0.98, 0.03, 0.22)	(-0.4, 0.88, 0.27)	(-0.15, -0.44, 0.89)
5	Cone Angle	22	16	15
5	Goal Angle	13	29	28

The mean axis is the average rotation axis over all trials for this particular condition.

The cone angle is the semi-vertical angle of cone expanded from mean vector to minimum size which includes 68% of orientations.

The goal angle is the angle of the mean axis to the goal direction, which is either (1, 0, 0), (0, 1, 0), or (0, 0, 1).

Fig. 9 shows the actual axis of rotation during the trials, calculated using the procedure outlined in section III.H. The plot shows that overall subjects were able to rotate around an axis that is similar to the goal axis; the overall average deviation from the goal axis is 28 degrees. As shown in Table 9, the rotation axis connected to the small object trials was closer to the goal axis for the Y and Z rotations. Results are displayed for the two object size trials separately for a more granular analysis. Regarding the X rotation trials, the rotation axes are all shifted towards having a positive z component in the vectors and usually towards having a positive y component as well. When increasing the number of digits the rotation axis shifts closer to the goal axis. The Y trials (neglecting the problematic 2 digit case) all have a negative x and positive z components. Finally, the Z trials show overall a narrower spread, and for those trials the small object is closer to the goal axis compared to the large object. All axes are shifted towards having negative x and y components and when increasing the number of digits the angle to the goal axis decreases.

V. DISCUSSION

Overall, for both the translational and rotational parts of the study, there exists a substantial degree of variation between subjects, suggesting that there is no 'hard limit' on the workspace ranges and that soft factors such as strategy, training, and confidence may play a significant role in human precision manipulation performance. Variation persisted despite scaling the object diameter to hand dimensions. Depending on the will of the participants to get closer to their limits and their ability to perform unintuitive motions, the workspaces can increase. This is also important for robotic systems, where an on-line

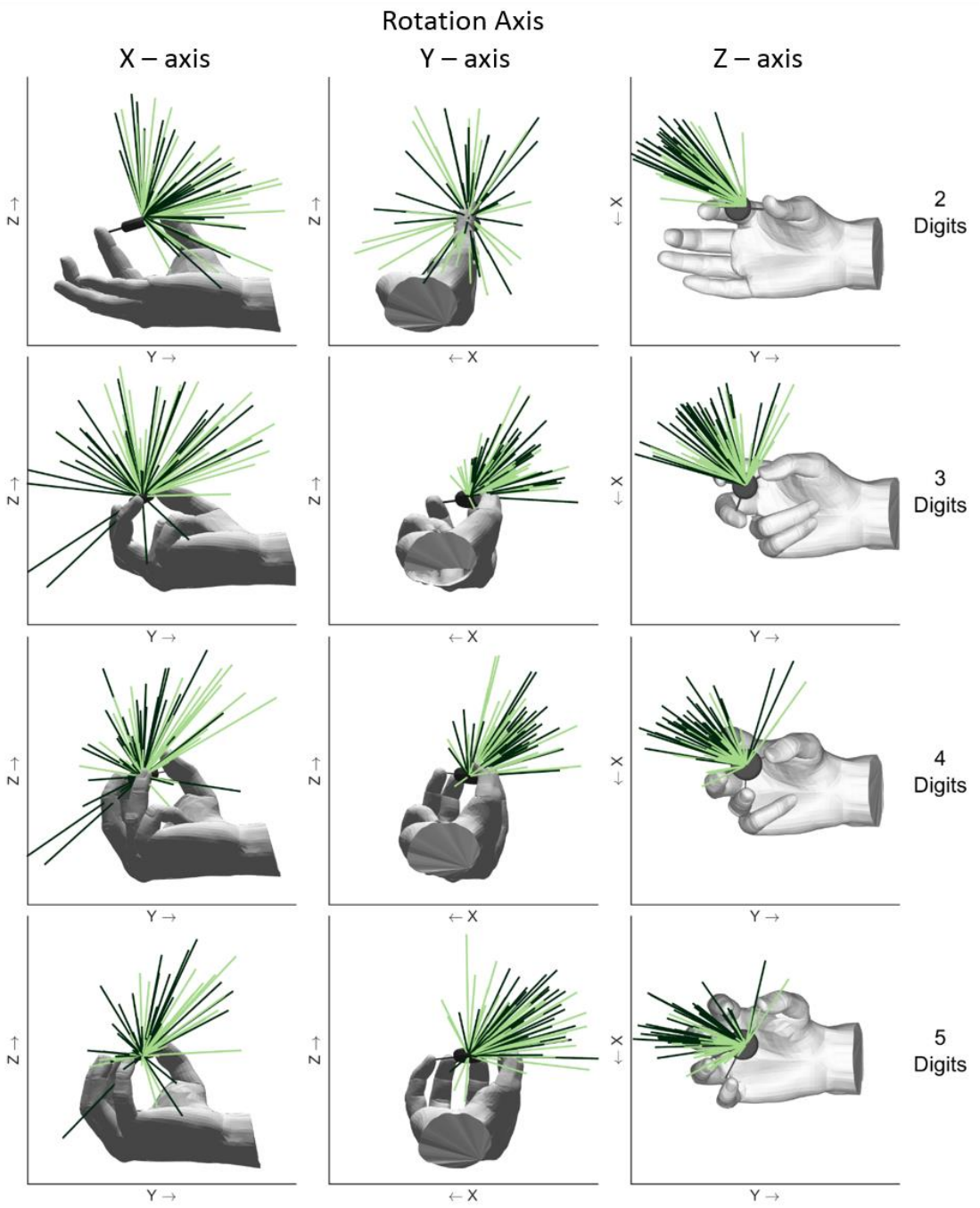

Figure 9. Orientations of the actual rotation axes about which the object was rotated is displayed; calculations are outlined in section III.H. Each line represents the mean rotation axis of one trial. Light color axes represent the 50mm object and dark color axes represent the 80mm object. The plots are oriented in such a way that the instructed goal axis is perpendicular to the page; hand models are included for reference, but are not representative of the actual hand shape during those trials. All lines intersect at the origin and have equal length. Each panel corresponds to a separate rotation task and are not to be interpreted as different views of the same task.

system of evaluating stability, such as from a slip sensor, could help in working closer to the hard workspace limits without dropping the object. Without feedback, a larger safety margin is likely required, which would reduce the useable workspace. While we instructed subjects to keep their contact location constant, they were unable to avoid some change of contact location during the course of the trial. Subjects usually reacted to those changes by either altering their exploration or by repositioning the object (in the rotation trials). Presently, robotic systems are mainly unable to react to those subtle changes. Stabilization should nonetheless not be overlooked, and in some cases small range of motion, coupled with mechanical gain, could suffice for various tasks, as in the example of writing with a pen. During active tool use, when the hand experiences large external torques, stiffness [24], slipping [25], and finger placement [23] certainly play an important role, and should be considered alongside the number of digits. For a quantification of stability during precision in-hand manipulation tasks, such as the ones in this experiment, readers should turn to [34].

While we suspected the length of the hand to be a significant factor, it is only significant for the rotational trials; it is positively correlated with the three rotational ranges. The reverse is true for hand width where a wider hand has an adverse effect on translational volume but has no statistically significant effect on rotational range. The size of the object relative to the hand was statistically significant in all rotation but not translation trials. It did however have a statistically significant effect on the translation range in the Z-direction. It should therefore be expected that smaller objects can be rotated further than larger ones, while larger objects can enable larger translation in the Z-direction. Therefore, a longer thinner hand is more likely achieve the largest overall translational and rotational workspace. This also suggests that when attempting to account for different hand sizes, hand length alone may not be enough and that hand width should be considered as well. Given the increased difficulty of manipulating objects much larger or smaller than the hand, we suspect that the regression trends would reverse had we included a larger range of object sizes in the experiment. Therefore, the trends should only be considered within the range of relative object sizes we tested.

Given that hand dimensions have been linked to sex [35] , by accounting for hand length and width, we were hoping to eliminate the effect of sex on the translational and rotational workspaces. Despite the effect of sex being statistically insignificant, some effect persisted. This suggests that there might be additional unaccounted factors that could be explored in future efforts.

When accounting for other factors, as well as randomizing the rotation tasks, trial order was not significant, however, positive relationships between trial order and the workspaces persisted, and thus could potentially be a limitation in the experiment. Another limitation is wrist movement. While subjects were instructed to minimize wrist motion, it was impossible to ensure without hindering the free motion of the fingers. Wrist posture plays a role in the range of motion and forces our fingers apply [36] and should be addressed in the future in order to obtain more accurate results.

A. Translation Experiment

The study of translational workspaces shows that with additional digits the workspaces decrease. Our study also found this trend with two different object sizes, therefore this seems to be a generalizable trend. However, it is not always statistically significant when going from one digit case to another. Differences are generally significant when comparing the 2 digit cases to most of the other 3-5 digit cases. One probable cause is that additional digits add constraints to the system and therefore the workspace is reduced. For a purely kinematic system, such as a parallel platform, the translational workspace will always decrease. It is difficult to assess how much the kinematic workspace will decrease by however, since in the four finger parallel platform case, adding an extra finger might not add any significant constraint.

This increase in constraint could potentially also be beneficial. Stability for example, will most likely increase and subjects will be able to explore larger proportions of their kinematic workspace. Additionally, it could prevent the objects from slipping at the fingertip, as occasionally occurred during the trials; digit–object contact locations usually drifted over the course of the experiment, sometimes to a point where subjects would drop the object or their motion would become more limited. Grasping the object with many fingers could allow for slight reset of the contact locations and thus enable a better exploration of the workspace. These results are relevant for robotic in-hand manipulation as it shows that even with grasps of up to five digits substantial in-hand translation motions can be achieved. Given the added potential stability, using more digits could be of great benefit for certain tasks. However, the results clearly show a tradeoff of a much smaller translational workspace as more fingers are utilized.

The results of the PCA analysis of the shape of the translation point clouds in Fig. 6 show that the direction of PC1 changes with the number of digits. In particular, the axis gradually shifts towards the pinky when adding fingers. It appears that the major direction of motion is generally pointed towards the center of the digits in contact with the object. So while it is possible to reduce the number of degrees of freedom in a robotic hand while maintaining a similar workspace [37], given that the major exploration direction changes with the number of digits, it shows that for robotic in-hand manipulation it may be more important to adapt the exploration procedures to the number of digits. The human summary data in the Appendix (Table A5) presents the summary of the PCA analysis of the workspace data that can be used either in design of artificial hands or as benchmark data against which performance can be compared.

B. Rotation Experiment

For the measurement procedure we deliberately chose a one dimensional exploration strategy for two reasons. First, our previous study using spherical objects [14] found a large inter-subject variation and we hoped to reduce this by simplifying the goal. Second, visualizing three dimensional rotations is non-intuitive and would be difficult for subjects to understand and likely decrease their ability to explore their full workspace. The coefficient of variation results show that the one-dimensional exploration did, in fact, reduce the spread. Excluding the two highest 2 digit coefficients, all coefficients of variation of the rotation trials are smaller than all translation coefficients.

The rotation manipulation results for the two digit case are somewhat problematic when grouped with the others, as the rotation of the object around the axis of the contact points cannot be controlled due to the nature of only two contacts. However, we felt that the two digit case is still important to investigate, so we chose to perform that condition nonetheless. In particular the Y-axis rotation may be inaccurate, since the uncontrollable axis is almost parallel to the Y-axis. This is the reason why it produced very small rotation amplitudes. Even though we did explain this problem to the subjects, to avoid introducing any bias, several subjects commented that the 2 digit, Y-axis rotation task is difficult or impossible. This is also why the 2 digit Y-axis condition, in particular, frequently exhibited different trends.

Compared to the translational workspaces, the rotation amplitudes present a different picture. X-axis and Z-axis

rotations, were found not to be dependent on the number of digits. The motions of the individual digits in these cases are similar – all move synchronously in the same direction. The constraints of adding an additional finger might be small and offset by added stability. The Y-axis rotation requires a different movement scheme: for example in the three digit case, the index finger has to flex, whereas the middle finger has to extend in order to rotate the object. This scheme also explains why the rotation amplitude is reduced when fingers are added. Due to the larger effective radius of the object, a similar translation of the digits results in a smaller rotation of the object.

Regarding the translational components from Fig. 8, the results show that for all trials subjects were not able or did not purely rotate the object. There always existed a certain amount of object translation associated with the motion. In particular, the 2 digit cases showed large relative translations, having the largest PC1 length and smallest rotation amplitudes. This might be partly due to the fact that fully controlling a 3D rotation with two digits is problematic, as there is always the uncontrollable degree of freedom around the axis of the object contact points. These results highlight the fact that in order to fully control the 6 DOF pose of an object more than 2 digits have to be used. Among other applications, this is important in haptic devices, which should be designed to use more than 2 digits. Adding extra fingers however, can lead to smaller translational workspaces, so tradeoffs between translational and rotational motions must be considered.

The actual axes of rotation, as presented in Fig. 9 and Table 9 show that subjects were often able to rotate the object around axes similar to the goal axis. Interestingly, the variation is not centered on the goal axis, but the mean is often rather different than the goal axis. This might indicate that those rotation axes are more intuitive or easier to perform than a pure rotation around the goal axis. Alternatively, it could also be a result of "enslaving", where fingers are either neurologically or physiologically interdependent or kinematically constrained to operate in concert [38]–[40]. This effect is evident in particular for rotations around the Z-axis (perpendicular to the palm), where the actualized mean axis of rotation is up to 40 degrees tilted away from the goal axis, but the actual spread between subjects is very small. The results are directly relevant for anthropomorphic robotic hands, where it might be beneficial to try to rotate objects around the mean axis we observed rather than the goal axis. The current analysis of the actual rotation angles only looks at the rotation from one extreme position to the other and assumes a direct rotation that connects the two orientations. In reality however, subjects might perform a more complex motion, which we plan to investigate in the future.

VI. Conclusion

The present work focuses on studying the effects of varying the number of digits used on the resulting manipulation abilities, in terms of translational workspaces and rotational ranges, by manipulating two circular objects, 50 and 80 mm in diameter. The overall average recorded volume for translational workspace is 5.1 cm^3, after scaling to a 17.5 cm hand length. The manipulation volume for five digits was less than half the two-digit (thumb-index) volume ($p < 0.001$) and the object sizes were not found to significantly influence the workspace volume. The average rotational range achieved over all conditions was 55 degrees, with the largest mean rotation of 88 degrees for the three-digit (thumb-index-middle) case around the distal-proximal axis. Rotation range around the ulnar-radial and dorsal-palmar axes was not found to significantly change with the number of digits. Rotation around the distal-proximal axis is affected by the number of digits. Analyzing the axis of rotation shows that on average the real axis of rotation was 28 degrees away from the goal axis and that there are consistent offsets from the axis, indicating preferred axes of rotation by the subjects.

Considering the points discussed above, one takeaway from this study that is particularly relevant to robotic manipulation research is the overall trend in precision manipulation performance as a function of the number of fingers utilized. In general, the results show a significant reduction in precision manipulation workspace volume and rotation range as the number of digits utilized increases from two to five for five of the six translation conditions and two of the six rotation conditions, suggesting that for these particular metrics, more fingers lead to a reduction in performance. In terms of kinematics, this seems to indicate that adding fingers does more in terms of adding constraints that limit motion than it does in adding degrees of freedom that increase force and motion capabilities (that might, for instance, be able to push objects further in directions limited by the active range of motion of other digits). Furthermore, while two digits (thumb-index) give the largest overall workspaces (or tied for largest) for five of the six rotation conditions, the lack of ability to control rotation in the distal-proximal direction suggests that three digits (thumb-index-middle) may be more desirable for overall precision manipulation capability.

These results must be taken with a grain of salt, however, as they only examine a portion of overall hand function. There are additional types of within-hand motions that we did not examine (such as finger-gaiting and movements that utilize sliding and rolling at the contacts), how number of fingers affect static grasping function, as well as how they affect other important metrics such as force production and grasped object stability. Furthermore, while we have shown how workspace sizes change with the number of digits used, the exact mechanism that influences those workspaces is still unknown. Are the added kinematic constraints the limiting factor in those trials, or perhaps the limitations on controllability of digits and forces play a larger role? Full hand modeling approaches might help to answer those questions.

The current study provides many insights into the translation and rotation capabilities of the human hand, and it will be valuable for the robotics community in a number of ways. It provides general benchmark data on the human in-hand manipulation performance and therefore gives first indications for what sizes of workspaces one might expect. Furthermore, for anthropomorphic hands, the information on the shape and alignment of those workspaces will aid in implementing those motions in an artificial hand. Finally, by better understanding human manipulation behavior, human-robot mapping and observing human motion can be improved.

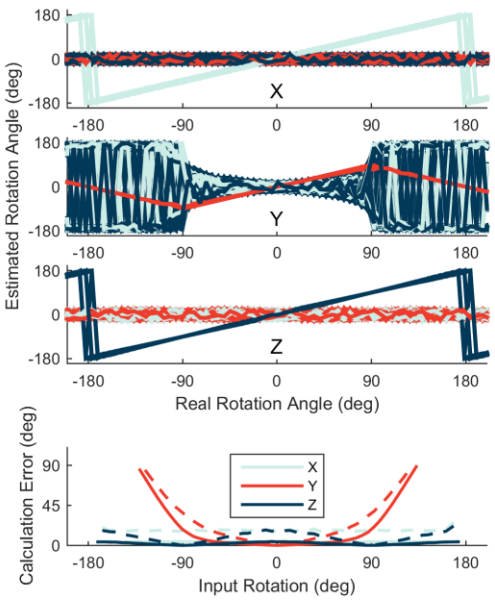

Figure A1. Error Estimation of the rotation angle calculation. For each coordinate, the real rotation matrix is multiplied with rotations around the two other axis with a random error of a certain magnitude. The top three plot show the estimated rotation angle for the three axes with an error magnitude of 20 degrees. The bottom plot shows the 90 percentile difference between the actual rotation and the calculated rotation for two error magnitudes (solid line 20 deg, dashed line 40 deg). The rotation estimation is influenced by the secondary rotations, however their influence is smaller than their magnitude. X and Z rotations are stable from almost -180 to 180 degrees, whereas Y is stable in an interval of less than [-90,90], depending on the amount of noise.

VII. Appendix

Please refer to the main text for context behind Fig. A1 and A2. Fig. A3 and A4, in contrast to Fig. 5, correspond to ANOVA tests performed between distributions separated by object size. Fig. A5 is the complementary analysis to Fig. 5 where relative object size is the ratio between the object diameter and hand length rather than hand width. Likewise, Tables A1-A4 complement Tables 2-5, where relative size is the ratio between the object diameter and hand length rather than hand width. Table A5 summarizes the PCA analysis of the translation workspace data. Tables A6-A8 complement Tables 6-8 in that they include both hand length and width and are used to identify which of the two has a significant effect for each rotational workspace. Fig. A6, in contrast to Fig. 7, corresponds to ANOVA tests performed between distributions separated by object size.

Acknowledgment

The authors would like to thank Dr. Nicolas Rojas for discussions relating to the rotation experiment and calculations of rotation angles.

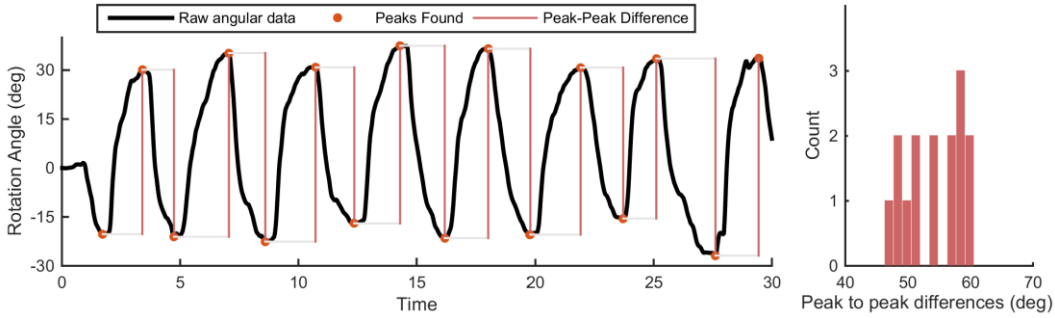

Figure A2. Left plot shows the raw data around the primary rotation, the peaks found in the data, and the peak-to-peak differences that were calculated. The right plot shows a histogram of the peak-to-peak differences. For visualization purposes a trial with few peaks (16) was chosen. The fastest trials have up to 90 peaks.

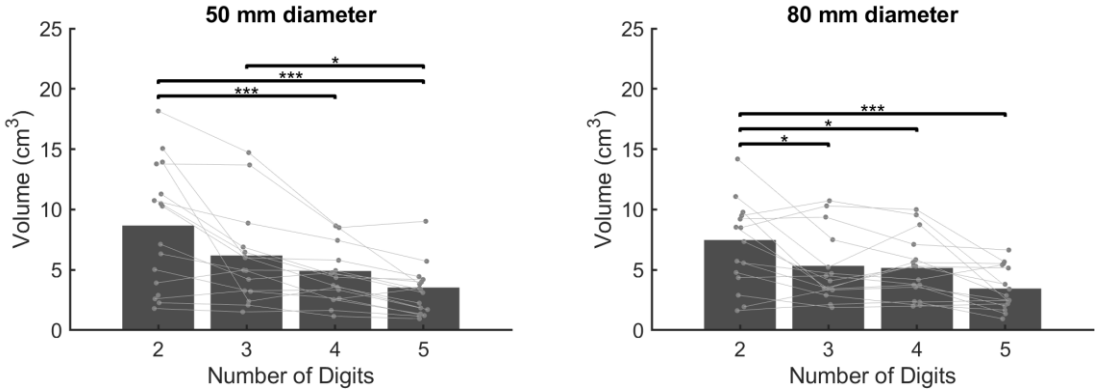

Figure A3. Volume vs. number of digits. The bar represents the mean workspace for each digit and diameter conditions. Grey lines connect the trials by the same subject and statistically significant reductions in volume are indicated, where * denotes $p<0.05$, ** denotes $p<0.01$, and *** denotes $p<0.001$ (single factor analysis of variance (ANOVA)). The difference in volume between the 50 mm and 80 mm object cases was not found to be significant if the number of digits is kept the same (further verified with a two-sided t-test for each number of digit condition). Following this initial test, a multiple comparison procedure was performed with the same Holm-Bonferroni correction applied to the p-values to test pairwise whether the means are equal. For the 50 mm diameter object, significant differences are present between the two digit case and the four and five digit cases, with $p<0.001$. A significant difference also exists between the 3 and 5 digit cases, with $p=0.035$. The median workspace volume for two digits (7.12 cm^3) is more than double the median volume for the five digit case (3.24 cm^3).

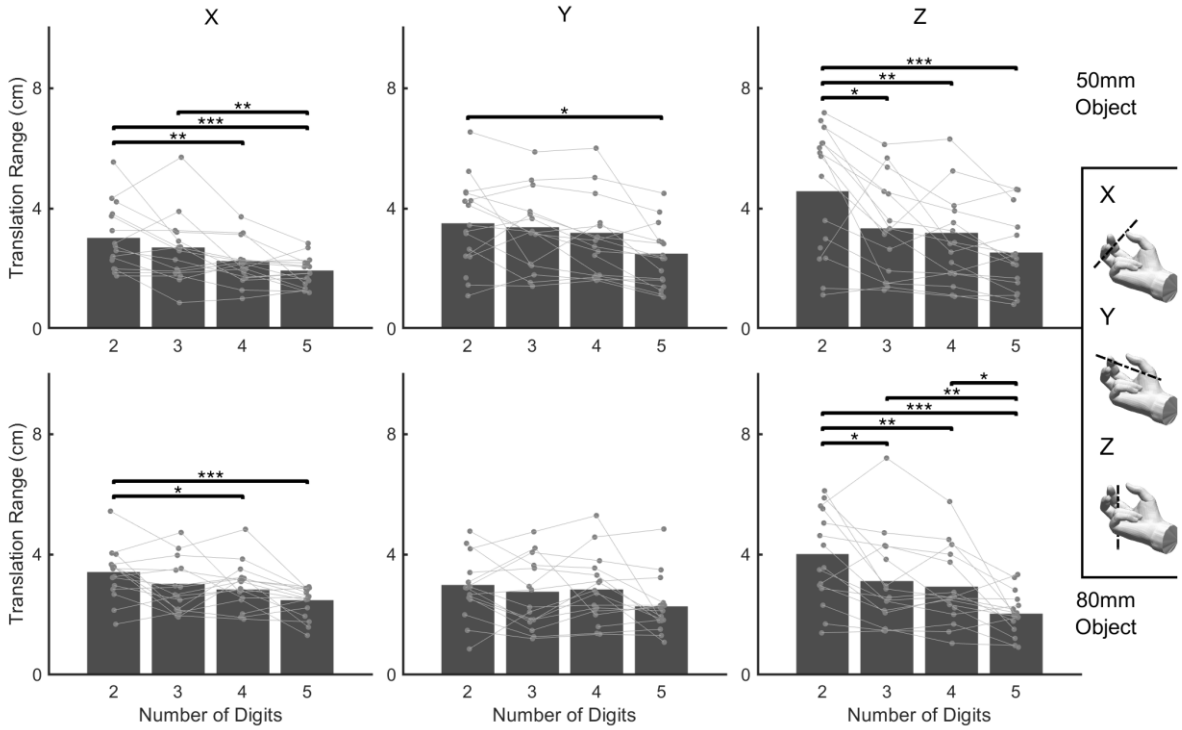

Figure A4. Overview of the translational ranges. For each 3D translation exploration trial, the ranges along the three major hand axes are calculated. The lines connect the results of a particular subject for one block. The three hand images on the right indicate the coordinate axes. The top row corresponds to the 50 mm object, whereas the bottom row corresponds to the 80 mm object. The significance levels for the differences between the number of digits is given in the image. * denotes $p<0.05$, ** denotes $p<0.01$, and *** denotes $p<0.001$ (single factor analysis of variance (ANOVA)). The effect of digits is partly significant in the X and Y directions, while most significant in the Z direction.

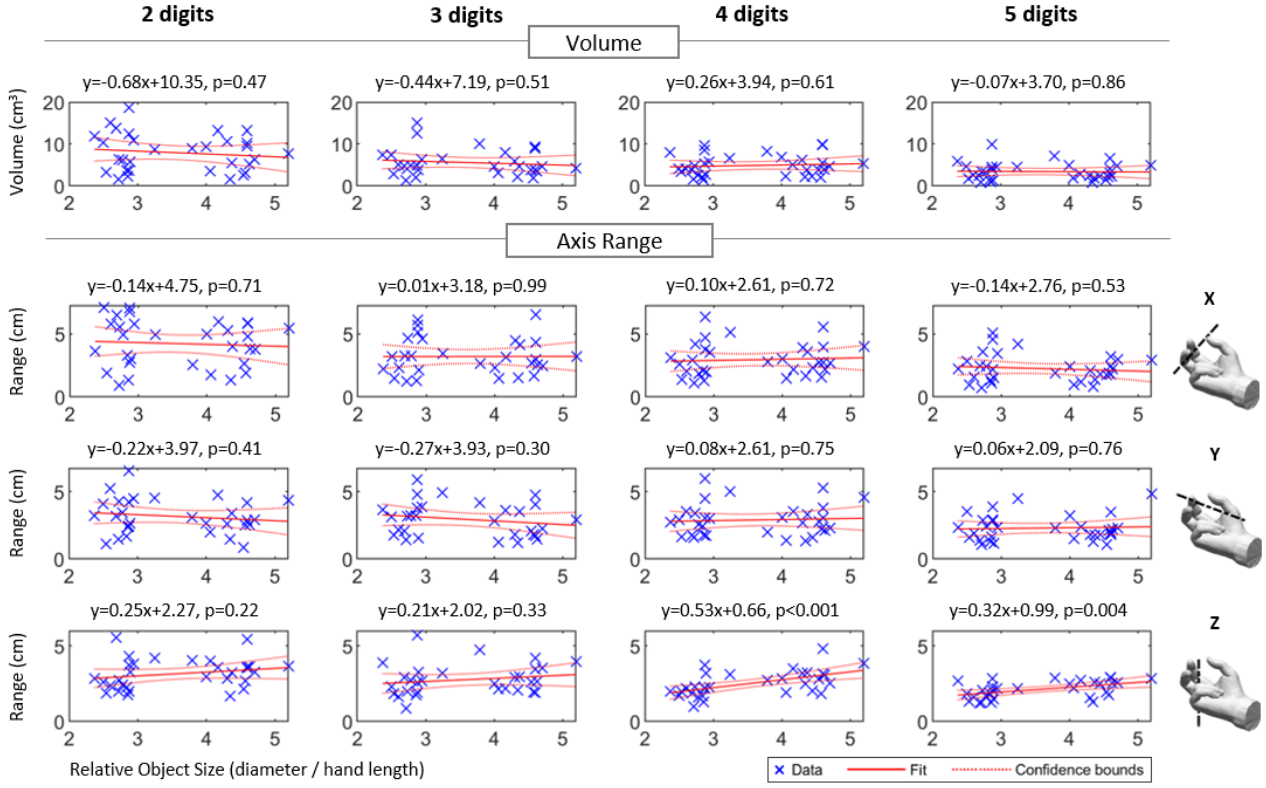

Figure A5. Overview of the translational workspace analyzed using both volume and range vs. relative object size (using hand length). The top row corresponds to the volume, whereas the bottom three rows correspond to range. For each 3D translation exploration trial, the ranges along the three major hand axes are calculated. The three hand images on the right indicate the coordinate axes. The significance levels for the differences between pairs of distributions of trial conditions is given in the image: * denotes $p<0.05$, ** denotes $p<0.01$, and *** denotes $p<0.001$. For each trial condition, a regression is displayed in Fig. 5 in the text.

TABLE A1
ANALYSIS OF COVARIANCE: TRANSLATION VOLUME

volume ~ 1 + sex + relative object size + trial # + # of dig.

	SumSq	df	MeanSq	F	p-value	partial η^2	adjusted p-value
sex	7.62	1	7.62	0.776	0.380	0.006	0.760
relative size	0.041	1	0.041	0.004	0.949	3.5e-5	0.949
trial number	36.9	1	36.9	3.76	0.055	0.031	0.164
# of digits	305.6	3	101.9	10.4	4.1e-6	0.209	1.6e-5
Error	1158.3	118	9.82				

Number of observations: 125, Root Mean Squared Error: 3.13
R-squared: 0.246, Adjusted R-Squared: 0.208
F-statistic vs. constant model: 6.41, p-value = 7.18e-06

TABLE A2
ANALYSIS OF COVARIANCE: X-DIRECTION TRANSLATION RANGE

range X ~ 1 + sex + relative object size + trial # + # of dig.

	SumSq	df	MeanSq	F	p-value	partial η^2	adjusted p-value
sex	11.2	1	11.2	5.76	0.018	0.046	0.054
relative size	0.408	1	0.408	0.210	0.648	0.002	0.648
trial number	8.99	1	8.99	4.63	0.034	0.038	0.067
# of digits	57.2	3	19.1	9.82	7.9e-6	0.200	3.2e-5
Error	229.3	118	1.94				

Number of observations: 125, Root Mean Squared Error: 1.39
R-squared: 0.271, Adjusted R-Squared: 0.234
F-statistic vs. constant model: 7.33, p-value = 1.13e-06

TABLE A3
ANALYSIS OF COVARIANCE: Y-DIRECTION TRANSLATION RANGE

range Y ~ 1 + sex + relative object size + trial # + # of dig.

	SumSq	df	MeanSq	F	p-value	partial η^2	adjusted p-value
sex	0.504	1	0.504	0.375	0.541	0.003	1
relative size	0.175	1	0.175	0.130	0.719	0.001	1
trial number	7.47	1	7.47	5.56	0.020	0.045	0.080
# of digits	12.3	3	4.10	3.06	0.031	0.072	0.093
Error	158.5	118	1.34				

Number of observations: 125, Root Mean Squared Error: 1.16
R-squared: 0.122, Adjusted R-Squared: 0.0769
F-statistic vs. constant model: 2.72, p-value = 0.0164

TABLE A4
ANALYSIS OF COVARIANCE: Z-DIRECTION TRANSLATION RANGE

range Z ~ 1 + sex + relative object size + trial # + # of dig.

	SumSq	df	MeanSq	F	p-value	partial η^2	adjusted p-value
sex	0.029	1	0.029	0.043	0.836	3.6e-4	0.960
relative size	9.64	1	9.64	14.3	2.5e-4	0.108	7.4e-4
trial number	0.338	1	0.338	0.502	0.480	0.004	0.960
# of digits	16.8	3	5.61	8.32	4.6e-5	0.174	1.8e-4
Error	79.5	118	0.674				

Number of observations: 125, Root Mean Squared Error: 0.821
R-squared: 0.259, Adjusted R-Squared: 0.221
F-statistic vs. constant model: 6.87, p-value = 2.85e-06

TABLE A6
ANALYSIS OF COVARIANCE: X-AXIS ROTATION RANGE

range X~ 1 + sex + hand len. + hand wid. + trial # + diameter + # of dig.

	SumSq	df	MeanSq	F	p-value	partial η^2	adjusted p-value
sex	1346	1	1346	5.83	0.017	0.045	0.688
hand length	1984	1	1984	8.60	0.004	0.065	0.020
hand width	1340	1	1340	5.81	0.017	0.045	0.688
trial number	5.22	1	5.22	0.023	0.881	1.4e-4	0.881
diameter	3063	1	3063	13.3	4.0e-4	0.097	0.002
# of digits	1034	3	345	1.49	0.220	0.035	0.439
Error	28388	123	231				

Number of observations: 132, Root Mean Squared Error: 15.2
R-squared: 0.216, Adjusted R-Squared: 0.165
F-statistic vs. constant model: 4.23, p-value = 0.000165

TABLE A7
ANALYSIS OF COVARIANCE: Y-AXIS ROTATION RANGE

range Y~ 1 + sex + hand len. + hand wid. + trial # + diameter + # of dig.

	SumSq	df	MeanSq	F	p-value	partial η^2	adjusted p-value
sex	2292	1	2292	5.94	0.016	0.046	0.055
hand length	5248	1	5248	13.6	3.4e-4	0.100	0.002
hand width	2407	1	2407	6.23	0.014	0.048	0.055
trial number	48.9	1	48.9	0.127	0.723	0.001	0.723
diameter	2328	1	2328	6.03	0.015	0.047	0.055
# of digits	58073	3	19358	50.1	3.1e-21	0.550	1.9e-20
Error	47507	123	386				

Number of observations: 132, Root Mean Squared Error: 19.7
R-squared: 0.601, Adjusted R-Squared: 0.575
F-statistic vs. constant model: 23.1, p-value = 2.87e-21

TABLE A8
ANALYSIS OF COVARIANCE: Z-AXIS ROTATION RANGE

range Z~ 1 + sex + hand len. + hand wid. + trial # + diameter + # of dig.

	SumSq	df	MeanSq	F	p-value	partial η^2	adjusted p-value
sex	150	1	150	0.651	0.421	0.005	1
hand length	5201	1	5201	22.6	5.4e-6	0.155	3.3e-5
hand width	55.0	1	55.0	0.239	0.626	0.002	1
trial number	99.0	1	99.0	0.430	0.513	0.004	1
diameter	4014	1	4014	17.5	5.5e-5	0.124	2.8e-4
# of digits	1864	3	621	2.70	0.049	0.062	0.194
Error	28287	123	230				

Number of observations: 132, Root Mean Squared Error: 15.2
R-squared: 0.32, Adjusted R-Squared: 0.276
F-statistic vs. constant model: 7.23, p-value = 7.89e-08

TABLE A5
SUMMARY STATISTICS OF THE PCA FIT

50 mm Object

Data	2 Digits	3 Digits	4 Digits	5 Digits
Workspace Centroid[1]	(-5.1±0.4, -5.6±0.3, 6.7±0.3)	(-4.4±0.3, -5.5±0.4, 7.4±0.3)	(-3.8±0.3, -5.6±0.3, 7.5±0.2)	(-3.4±0.3, -5.7±0.3, 7.3±0.2)
PC1 vector / PC1 cone angle[2]	(0.0, 1.2, 2.3) / 43 °	(-0.5, 1.4, 1.5) / 39 °	(-0.5, 1.2, 1.4) / 27 °	(-0.8, 0.8, 1.0) / 36 °
PC2 vector / PC2 cone angle[2]	(0.7, -0.3, 0.9) / 48 °	(0.5, -0.1, 0.8) / 42 °	(0.4, -0.1, 0.7) / 37 °	(0.2, 0.0, 0.6) / 51 °
PC3 vector / PC3 cone angle[2]	(-0.3, -0.3, 0.3) / 27 °	(-0.2, -0.3, 0.2) / 31 °	(-0.2, -0.3, 0.3) / 39 °	(0.0, -0.1, 0.3) / 71 °

80 mm Object

Data	2 Digits	3 Digits	4 Digits	5 Digits
Workspace Centroid[1]	(-5.4±0.3, -6.0±0.3, 6.3±0.2)	(-4.9±0.4, -5.9±0.3, 6.9±0.2)	(-4.3±0.3, -5.9±0.3, 6.9±0.1)	(-3.7±0.3, -6.3±0.3, 6.6±0.3)
PC1 vector / PC1 cone angle[2]	(0.4, 0.5, 2.1) / 52 °	(0.4, 0.3, 1.8) / 67 °	(-0.6, 0.8, 1.4) / 57 °	(-0.7, 0.7, 0.8) / 40 °
PC2 vector / PC2 cone angle[2]	(0.4, 0.2, 1.2) / 66 °	(0.3, 0.2, 0.8) / 40 °	(0.3, 0.2, 0.8) / 41 °	(0.2, -0.0, 0.7) / 40 °
PC3 vector / PC3 cone angle[2]	(-0.2, -0.3, 0.2) / 19 °	(-0.2, -0.3, 0.2) / 22 °	(-0.1, -0.2, 0.3) / 45 °	(-0.0, -0.1, 0.4) / 75 °

Length units in cm are based on a 17.5 cm length hand. All three element values are given in (ulnar, proximal, palmar) coordinates relative to the base frame skin sensor one-third of the way from the continuation of the wrist flexion crease to the bump from the fourth metacarpal head, along the fourth metacarpal (See Fig. 2).

1 95% confidence interval based on standard error of the mean for each individual coordinate.

2 Semi-vertical angle of cone expanded from mean vector to minimum size which includes 68% of orientations.

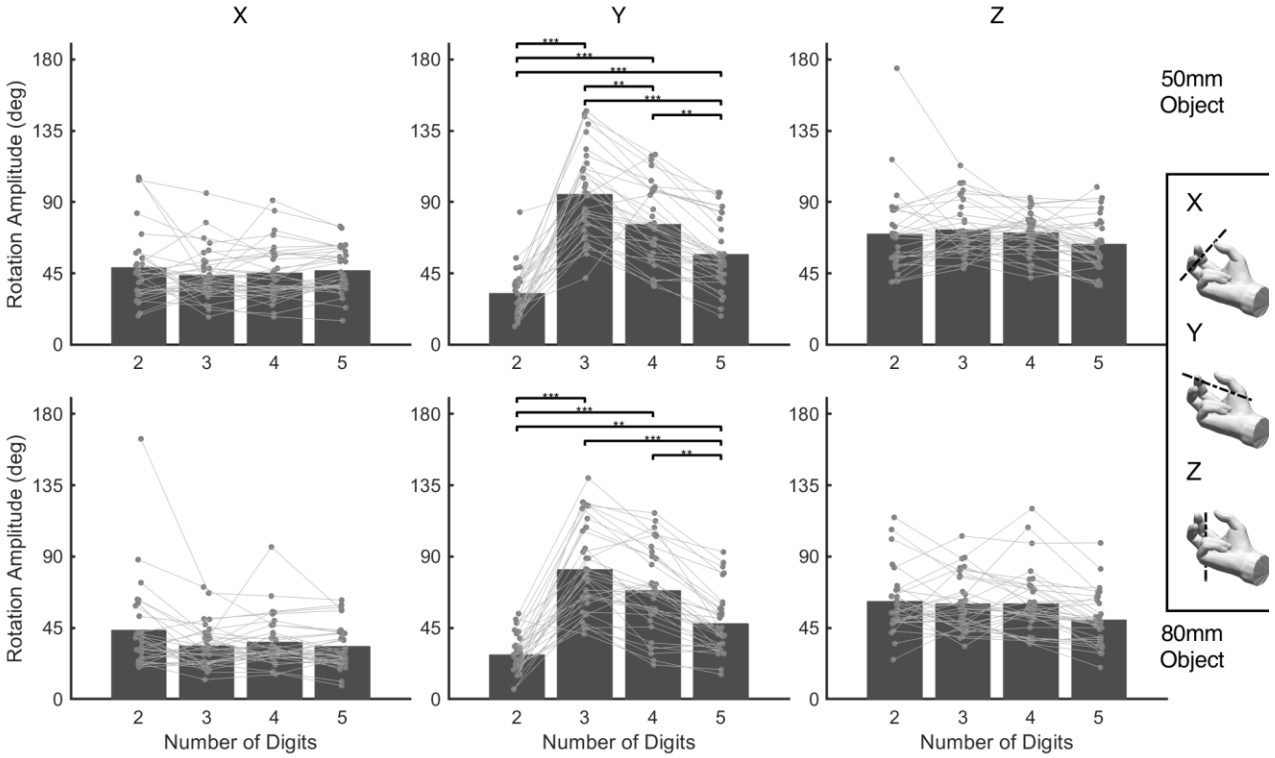

Figure A6. Overview of the rotational ranges for all 24 conditions. The lines connect the results of a particular subject for one block. Each bar represents the mean value for the trial. The significance levels for the differences between number of digits is given in the image. The three hand images on the right indicate the directions of the three rotations in the experiment. The top row corresponds to the 50 mm object, whereas the bottom row corresponds to the 80 mm object. * denotes $p<0.05$, ** denotes $p<0.01$, and *** denotes $p<0.001$ (single factor analysis of variance (ANOVA)).

REFERENCES

[1] I. M. Bullock, R. R. Ma, and A. M. Dollar, "A Hand-Centric Classification of Human and Robot Dexterous Manipulation," *IEEE Trans. Haptics*, vol. 6, no. 2, pp. 129–144, 2013.

[2] S. A. Heldstab, Z. K. Kosonen, S. E. Koski, J. M. Burkart, C. P. Van Schaik, and K. Isler, "Manipulation complexity in primates coevolved with brain size and terrestriality," *Sci. Rep.*, vol. 6, no. March, pp. 1–9, 2016.

[3] M. J. Liu, C. H. Xiong, and D. Hu, "Assessing the manipulative potentials of monkeys, apes and humans from hand proportions: Implications for hand evolution," *Proc. R. Soc. B Biol. Sci.*, vol. 283, no. 1843, 2016.

[4] Y. Guan, H. Zhang, X. Zhang, and Z. Guan, "Workspace generation for multifingered manipulation," *Adv. Robot.*, vol. 25, no. 18, pp. 2293–2317, Jan. 2011.

[5] A. Bicchi, A. Marigo, and D. Prattichizzo, "Dexterity Through Rolling: Manipulation of Unknown Objects," *IEEE Int. Conf. Robot. Autom.*, no. May, pp. 1583–1588, 1999.

[6] K. Tahara, K. Maruta, and M. Yamamoto, "External sensorless dynamic object manipulation by a dual soft-fingered robotic hand with torsional fingertip motion," in *IEEE International Conference on Robotics and Automation*, 2010, pp. 4309–4314.

[7] H. Liu *et al.*, "Multisensory five-finger dexterous hand: The DLR/HIT hand II," in *2008 IEEE/RSJ International Conference on Intelligent Robots and Systems, IROS*, 2008, pp. 3692–3697.

[8] C. S. Lovchik and M. A. Diftler, "The Robonaut hand: a dexterous robot hand for space," in *Robotics and Automation, 1999. Proceedings. 1999 IEEE International Conference on*, 1999, vol. 2, pp. 907–912 vol.2.

[9] F. Lotti, P. Tiezzi, G. Vassura, L. Biagiotti, G. Palli, and C. Melchiorri, "Development of UB Hand 3: Early Results," in *Robotics and Automation, 2005. ICRA 2005. Proceedings of the 2005 IEEE International Conference on*, 2005, pp. 4488–4493.

[10] L. Biagiotti, F. Lotti, C. Melchiorri, and G. Vassura, "How Far is the Human Hand? A Review on Anthropomorphic End Effectors," 2004.

[11] I. M. Bullock, T. Feix, and A. M. Dollar, "Workspace Shape and Characteristics for Human Two- and Three-Fingered Precision Manipulation," *IEEE Trans. Biomed. Eng.*, vol. 62, no. 9, pp. 2196–2207, 2015.

[12] M. R. Cutkosky and R. D. Howe, "Human Grasp Choice and Robotic Grasp Analysis," in *Dextrous Robot Hands*, 1990, pp. 5–31.

[13] M. Santello, M. Flanders, and J. F. Soechting, "Postural Hand Synergies for Tool Use," *J. Neurosci.*, vol. 18, no. 23, pp. 10105–10115, Dec. 1998.

[14] I. M. Bullock, T. Feix, and A. M. Dollar, "Analyzing Human Fingertip Usage in Dexterous Precision Manipulation: Implications for Robotic Finger Design," *IEEE/RSJ Int. Conf. Intell. Robot. Syst.*, no. Iros, pp. 1622–1628, 2014.

[15] A. Bicchi, "Hands for dexterous manipulation and robust grasping: a difficult road toward simplicity," *Robot. Autom. IEEE Trans.*, vol. 16, no. 6, pp. 652–662, 2000.

[16] R. Zheng and J. Li, "Kinematics and workspace analysis of an exoskeleton for thumb and index finger rehabilitation," in *2010 IEEE International Conference on Robotics and Biomimetics, ROBIO 2010*, 2010, pp. 80–84.

[17] G. Guthart and J. S. Jr, "The Intuitive telesurgery system: overview and application," in *IEEE International Conference on Robotics and Automation*, 2000, pp. 618–621.

[18] V. Hayward and O. R. Astley, "Performance Measures for Haptic Interfaces," in *Robotics Research*, G. Giralt and G. Hirzinger, Eds. Springer London, 1996, pp. 195–206.

[19] T. Feix, I. M. Bullock, Y. Gloumakov, and M. D. Aaron, "Rotational Ranges of Human Precision Manipulation When Grasping Objects With Two to Five Digits," in *Engineering in Medicine and Biology Conference*, 2015.

[20] I. M. Bullock, T. Feix, and A. M. Dollar, "Human Precision Manipulation Workspace: Effects of Object Size and Number of Fingers Used," in *Engineering in Medecine and Biology Conference*, 2015.

[21] L.-C. Kuo, H.-Y. Chiu, C.-W. Chang, H.-Y. Hsu, and Y.-N. Sun, “Functional workspace for precision manipulation between thumb and fingers in normal hands.,” *J. Electromyogr. Kinesiol.*, vol. 19, no. 5, pp. 829–839, Oct. 2009.

[22] C. Chang and Y. Sun, “Learning-based estimation of functional workspace in cooperative fingers motion,” in *International Conference on Bioinformatics and Biomedical Technology*, 2012, vol. 29, pp. 141–145.

[23] J. Friedman and T. Flash, “Task-Dependent Selection of Grasp Kinematics and Stiffness in Human Object Manipulation,” *Cortex*, vol. 43, no. 3, pp. 444–460, 2007.

[24] V. M. Zatsiorsky and M. L. Latash, “Multifinger prehension: an overview.,” *J. Mot. Behav.*, vol. 40, no. 5, pp. 446–76, Oct. 2008.

[25] M. R. Cutkosky and I. Kao, “Computing and Controlling the Compliance of a Robotic Hand,” *IEEE Trans. Robot. Autom.*, vol. 5, no. 2, pp. 151–165, 1989.

[26] P. Cesari and K. M. Newell, “Body-scaled transitions in human grip configurations.,” *J. Exp. Psychol. Hum. Percept. Perform.*, vol. 26, no. 5, pp. 1657–1668, Oct. 2000.

[27] P. Cesari and K. M. Newell, “The scaling of human grip configurations.,” *J. Exp. Psychol. Hum. Percept. Perform.*, vol. 25, no. 4, pp. 927–935, 1999.

[28] R. Flanagan, M. Burstedt, and R. Johansson, “Control of Fingertip Forces in Multidigit Manipulation,” *J. Neurophysiol.*, vol. 81, no. 4, pp. 1706–1717, Apr. 1999.

[29] R. Gilster, C. Hesse, and H. Deubel, “Contact points during multidigit grasping of geometric objects,” *Exp. Brain Res.*, vol. 217, no. 1, pp. 137–151, Mar. 2012.

[30] O. Jasuja and G. Singh, “Estimation of stature from hand and phalange length,” *J. Indian Acad. Forensic Med.*, vol. 26, no. 3, pp. 100–106, 2004.

[31] N. Fisher, T. Lewis, and B. Embleton, *Statistical analysis of spherical data*, 1st ed. Cambridge, Great Britain: Cambridge University Press, 1987.

[32] M. Panjabi, M. Krag, and V. Goel, “A technique for measurement and description of three-dimensional six degree-of-freedom motion of a body joint with an application to the human spine,” *J. Biomech.*, vol. 14, no. 7, pp. 447–460, Jan. 1981.

[33] S. Holm, “A Simple Sequentially Rejective Multiple Test Procedure,” *Scand. J. Stat.*, vol. 6, no. 2, pp. 65–70, 1979.

[34] Y. Gloumakov, T. Feix, I. M. Bullock, and A. M. Dollar, “Object stability during human precision fingertip manipulation,” in *IEEE Haptics Symposium, HAPTICS*, 2016, vol. 2016-April.

[35] D. T. Case and A. H. Ross, “Sex Determination from Hand and Foot Bone Lengths,” *J. Forensic Sci.*, vol. 52, no. 2, pp. 264–270, 2007.

[36] M. S. Hallbeck, “Flexion and extension forces generated by wrist-dedicated muscles over the range of motion,” *Appl. Ergon.*, vol. 25, no. 6, pp. 379–385, 1994.

[37] D. Dragulescu, V. Perdereau, M. Drouin, L. Ungureanu, and K. Menyhardt, “3D active workspace of human hand anatomical model,” *Biomed. Eng. Online*, vol. 6, no. 15, pp. 1–12, 2007.

[38] V. M. Zatsiorsky, Z. M. Li, and M. L. Latash, “Enslaving effects in multi-finger force production,” *Exp. Brain Res.*, vol. 131, no. 2, pp. 187–195, 2000.

[39] M. H. Schieber and M. Santello, “Hand function: Peripheral and central constraints on performance,” *J. Appl. Physiol.*, vol. 96, no. 6, pp. 2293–2300, 2004.

[40] F. Paclet, S. Ambike, V. M. Zatsiorsky, and M. L. Latash, “Enslaving in a serial chain: Interactions between grip force and hand force in isometric tasks,” *Exp. Brain Res.*, vol. 232, no. 3, pp. 775–787, 2014.